The Stratigraphy of the New Tuli Basin Fossil Sites in Zimbabwe

Student Name: Michel Zondo

Student No: 2011093

ORCID No 0000-0002-7918-7028

Supervisors: Prof Jonah Choiniere, Mr Timothy Broderick, Mr Darlington Munyikwa

A dissertation submitted to the Faculty of Science, University of the Witwatersrand, Johannesburg, in fulfilment of the requirements for the degree of Master of Science.

THE STRATIGRAPHY OF THE NEW TULI BASIN FOSSIL SITES I N ZIMBABWE

MICHEL ZONDO

A dissertation submitted to the Faculty of Science, University of the Witwatersrand, Johannesburg, in fulfilment of the requirements for the degree of Master of Science.

Johannesburg, 2024

DECLARATION

I declare that this Masters project is my own unaided work, except as acknowledged in the text. Neither the substance nor any part of it has been submitted in the past or is being submitted for a degree in any other University. The information used in this Master of Science project was obtained by me through research work, during the period in which I was registered as a part-time student in the school for Geosciences.

M. Zondo

7th day of September 2024

ABSTRACT

This thesis investigated new fossil-bearing outcrops of the Mpandi Formation of Zimbabwe, exposed at Sentinel Ranch in the Tuli Basin, at sites named “Wedding Hill “and “Pimwe Hill”. The Mpandi Formation exposures at Sentinel Ranch reveal strata that were deposited in fluvial environments that occasionally experienced flooding in otherwise usually dry and hot climatic conditions. These fluvial systems deposited facies that are mostly dominated by fine sediments and their facies have similarities with those found in the main Karoo Basin of South Africa. The use of borehole data helped establish the thickness of the Mpandi Formation and the explorable portion of the formation was estimated to be around 54 metres. Detrital zircons collected from main Sentinel outcrops were used to estimate the maximum depositional age of the sediments using inductively coupled plasma mass spectrometer (LA-ICPMS) methods. Although sparse, the youngest zircons in these samples yielded ages of 199.2 ± 5.1 Ma and 200.8 ± 5.8 Ma, with error bars suggesting maximum depositional ages in the earliest Jurassic or possibly the latest Triassic. A bonebed at the Wedding Hill site produced many postcranial bones of sauropodomorphs, including the articulated leg of a very large individual sauropodomorph, and the first theropod bones recorded from the Mpandi Formation at Sentinel. The discoveries improve our knowledge of the fauna diversity of the Mpandi Formation, permitting more accurate biostratigraphic correlation and enhancing our understanding of the Triassic- Jurassic interval.

ACKNOWLEDGEMENTS

I am grateful to my Supervisor Professor Jonah N. Choiniere for his expert guidance throughout the duration of my studies. I trust it was not an easy task supervising a part-time student who only visited Wits for short periods of time, but he skilfully and patiently assisted me carry out all the tasks and availed useful publications. Gratitude is also extended to my project co supervisors Mr. Timothy Broderick and Mr. Darlington Munyikwa who were always there to assist. Thanks to Tim for providing some important historical publications which are not easy to find in libraries. I would like to thank Dr Lara Sciscio for assisting with sedimentological and stratigraphical aspects during fieldwork. I would also like to extend my thanks to Dr Kimi Chapelle who inspired me to embark on this study during our research fieldtrips to the Lake Kariba in the Zambezi Valley some few years ago. As a full-time worker of the Natural History Museum of Zimbabwe, I frequently needed time off to do my studies, and Dr Moira FitzPatrick as the Director of the institution was always supportive, I would like to pass my appreciation to her. I also like to convey my gratitude to PAST for providing funding for my studies. Appreciation also goes to the ESI fossil preparatory lab staff, especially Gladys Mokoma for preparing my specimens. Finally, I would like to thank my wife Nqobizitha and my children Simelokuhle and Sitholumusa for being supportive and understanding even during the times I could not be available to them.

Table of Contents

TABLE OF FIGURES

LIST OF TABLES

LIST OF APPENDICES

CHAPTER 1

INTRODUCTION

Purpose of study

The main goals of this study were:

- To describe the lithofacies and interpret the sedimentology at two bone-bearing localities (Wedding Hill and Pimwe Hill, respectively) of the Mpandi Formation of the Tuli Basin of Zimbabwe at Sentinel Ranch.
- To identify to the lowest taxonomic level possible, the fossil vertebrates preserved from these and other nearby localities in the same stratigraphic sequence.
- To assess similarities between these fauna and sediments with the upper Karoo strata of the main Karoo Basin (MKB).
- To determine maximum depositional ages of the Mpandi Formation using detrital zircon samples assessed with laser ablation – inductively coupled plasma mass spectrometer (LA-ICPMS) methodology.

Validation of the problem

The Tuli Basin, especially the Zimbabwean portion, has received little attention in palaeontological research, with the last publication issued by Rogers *et al* (2004) almost two decades ago. Since then, several notable fossil finds have been made in various localities resulting in the need for updated understandings. Historically, tetrapod fossils from the Tuli Basin were mostly assigned to *Massospondylus* and the now nomen-dubium taxon, *Euskelosaurus*, where determinations were usually influenced by taxon body size (McPhee *et al*., 2017) rather than based on shared homologous features. These two taxa formed the basis for the upper Karoo biozonation of the Main Karoo Basin (Kitching and Raath,1984), and respectively have long been thought to characterise sedimentary rocks laid down during the Early Jurassic and Late Triassic, respectively. Tremendous revisions have since occurred, since the pioneering work of Kitching and Raath, with recent studies showing that *Euskelosaurus* is no longer a valid taxon (McPhee *et al.,* 2017). The invalidation of the *Euskelosaurus* meant that the *Euskelosaurus* range zone could no longer be applicable, and the sediments required a revisit, and further study of fossils from the basin. The most recent revisions to main Karoo Basin biozonation have formally established the *Scalenodontoides* Assemblage Zone and *Massospondylus* Assemblage Zone, respectively representing Late Triassic and Early Jurassic time intervals (Viglietti *et al*, 2020a, 2020b).My Honours Degree project, established the presence of new taxa at the Sentinel Ranch locality in Zimbabwe's Tuli Basin, with evidence for co-occurrence in the main Karoo Basin, further necessitating the study of the stratigraphy of the Tuli Basin (Zondo, 2019).

Literature review of previous studies on related problem

The Tuli Basin, especially the Zimbabwean portion, has not received as much attention as the main Karoo Basin in South Africa with regards to research related to palaeontology. Most of the historical work in the Tuli Basin was largely inspired by the search for coal (Robertson, 1967; Thompson, 1975; Bordy, 2000; Rogers *et al*., 2004).

Basin development

A shallow-angle subduction of the Palaeo-Pacific plate at the southern coalescent edge of Gondwana, pushed it under the supercontinent. The resultant compressional forces in relation to collision and terrain up-lifting led to the formation of the Cape Fold Belt. The terrane up-lift served as precursory load that led to the formation of the Karoo retroarc foreland system, which comprises the main Karoo Basin, and the smaller basins to its north up to the Tuli Basin (Catuneanu *et al*., 2005). Both flexural and extensional tectonic forces acted in creating sediment accommodation in the Tuli Basin and the other basins in the Limpopo area (Light, 1982; Catuneanu *et al*., 2005). The flexural regime was responsible for the deposition of Permian to Carboniferous beds while the extensional regime was responsible for the deposition of the Triassic to Jurassic Stormberg Group equivalent beds in the Tuli Basin (Catuneanu *et al*., 2005).

Broderick (1979) noted an east-south-east- trending synclinal flexing and downfaulting of the Nuanetsi and Tuli synclines which controlled the deposition and prominence of the Karoo rocks. He reported the abundant occurrence of calcretes as surface deposits within the Limpopo Mobile Belt, and the occurrence of magnetite quartzite throughout the Central Zone of the Limpopo Mobile Belt. The geology of the eastern side of Beitbridge was elaborated and striking similarities of Nuanetsi Karoo sediments and those of the Tuli Basin were reported.

Location of the Tuli Basin and of the study area

The fault-bound syncline comprising the Tuli Basin is situated to the north of the main Karoo Basin and extends across the tripartite common borders of Botswana, South Africa, and Zimbabwe (Figure 1.1). The Karoo sequence is impressed upon rocks of the ENE-trending Limpopo Mobile Belt, lying between the Archaean Zimbabwe Craton to the north and the Kaapvaal Craton in the south. It forms the western part of a failed rift triple junction, that was initiated by the break-up of the supercontinent Gondwana (Bordy and Catuneanu, 2001; Rogers *et al*., 2004). The basin inclines in an east-west direction, between latitudes 28°,10′ E and 30°,30′ E, and it stretches for about 300 km (Bordy, 2000; Rogers *et al*.,2004). The Zimbabwean portion spreads between latitudes 29°,00′ E and 30°,30′ E. The study area is in Sentinel Ranch, a game reserve situated along the Limpopo River approximately 60km west of Beitbridge town. Sentinel Ranch is the main dinosaur-hosting locality in the southern part of Zimbabwe. Only the Mpandi and the Forest Sandstone formations (Figure 1.3) are exposed at Sentinel Ranch, with the former being the only fossil-bearing stratum (Rogers *et al*.,2004).

The Samkoto Formation (Cooper, 1981; Rogers *et al*., 2004 and in some early publications), is here referred to as the Forest Sandstone Formation, as similar formations in other basins in Zimbabwe are called (Thompson, 1975; Broderick, 1979). The name Forest Sandstone has been used for this formation before and its continued use could help to correlate these strata with ease across all the basins in the country. In this report, Forest Sandstone will be used in place of Samkoto Formation.

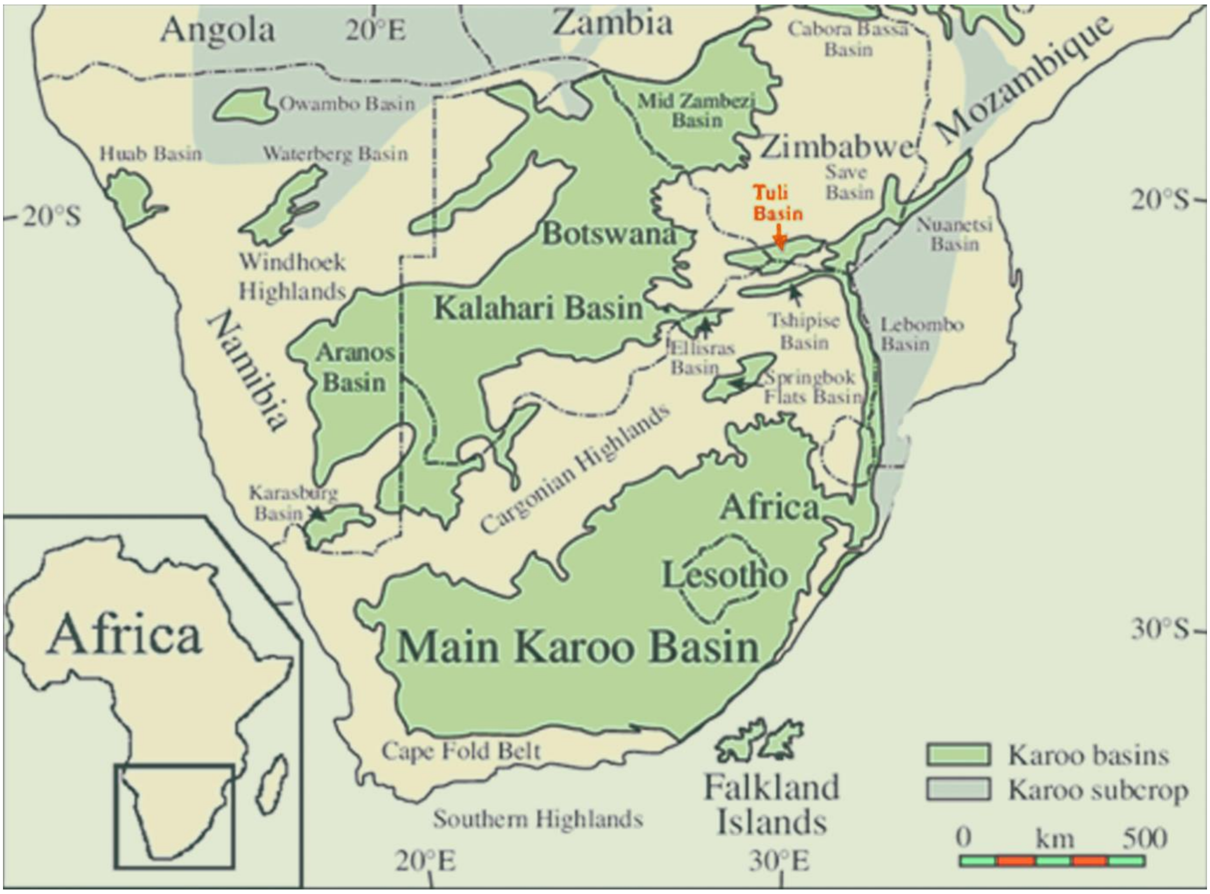

Figure 1.1. Map of the Karoo Basins of southern Africa, with the Tuli Basin situated to the north of the main Karoo Basin, spreading across the Borders of Botswana, South Africa, and Zimbabwe (modified after Catuneanu, 2005).

Geology, Stratigraphy and Palaeontology

The Tuli Basin preserves sedimentary and igneous rocks of the Karoo Supergroup, but its sequence is much thinner, with an estimated maximum sedimentary thickness of approximately 450- 500 m (Bordy, 2000; Bordy and Catuneanu, 2001; Rogers *et al*., 2004). The main Karoo Basin is extensive with a maximum thickness of 12 km for the sedimentary succession (Smith, 1995).

The Karoo sedimentary succession in the Tuli basin unconformably overlies Archaean gneisses of the highly metamorphosed Limpopo Mobile Belt. The metamorphosis of the gneisses was a consequence of the collision of the Zimbabwe and the Kaapvaal cratons (Light,1982). The Karoo Supergroup rocks have been preserved due to down-faulting of post-Karoo age. The Limpopo Mobile Belt is divided into three lithological sections, the North Marginal Zone (NMZ), Central Zone (CZ), and South Marginal Zone (SMZ).

The NMZ comprises mostly high-grade granite-greenstone terrain, the CZ comprises metasediments, s-type granitoid gneisses and anorthosite. The SMZ is associated with enderbitic and charnockitic gneisses (Khoza *et al*, 2013). The Tuli basin is fault bounded by a combination of NE-and ENE- trending fractures, together with minor fracturing on NW and N to NNE trend (Bordy, 2000; Rogers *et al*, 2004; Chinoda *et al*, 2009). A complete succession of sedimentation is shown by borehole logs, commencing with glacially deposited tillites of the Dwyka-age overlying the gneisses (Lister, 1987). The lithostratigraphic scheme structure of the Tuli Basin is as follows in ascending order: Dwyka diamictite, Fulton's Drift Mudstone. Gushu, Mpandi and Forest Sandstone formations (Table 1.1).

Overlying the Forest Sandstone Formation are olivine basalts overlain by a thick succession of Tuli tholeiites belonging to the Karoo Large Igneous Province (LIP). The Lower Karoo strata are exposed at some parts of the neighbouring Nottingham Ranch and to the east of Beitbridge (Broderick, 1979; Rogers *et al*., 2004).

This study mainly focusses on the Mpandi Formation from where numerous dinosaur fossils have been collected (Figure 1.2). The formation is sandwiched between the underlying Gushu Formation, basal to the Upper Karoo, and the overlying Forest Sandstone Formation. The Mpandi Formation comprises facies ranging from silty claystones to coarser grained sandstones with an alternating occurrence (Figure 1.3)

(Bordy, 2000; Rogers *et al*., 2004). The basal portions of the exposed Mpandi Formation are massive sandstones. Elsewhere bedding is very rare in sandstones though occasionally local faint trough cross bedding can be seen. The sandstones are quartz-rich and moderately sorted. These mostly red-to-light-grey facies occasionally host carbonate nodules and silicified root casts (Figures 1.5a, b, c), suggesting (fluvial/terrestrial) deposition in arid or semi-arid environments (Zamanian *et al*., 2016). The sandstones alternate with siltstones that host silicified root traces. Finer grained facies such as siltstones, claystones spotting calcareous nodules and concretions are interpreted as overbank deposits in semi-arid environments (Table 1.2). Occasionally there are pebbly /coarse to very coarse sandstones (Figure 1.5d), interpreted as deposition via high energy transient stream systems that experienced occasional flooding (Bordy, 2000; Rogers *et al*, 2004; Bordy & Eriksson, 2015). The Mpandi Formation attains a maximum thickness of approximately 30m of exposed outcrop within the study area (Rogers *et al*., 2004) while historical borehole information suggests it has a total thickness of up to 300m (Bordy, 2000), being some 190 m-thick in Borehole MRDI on Nottingham.

Despite earlier geological expedition activities in the Tuli Basin, the occurrence of fossil bones was not reported. It was in 1967 that a report on the discovery of fossil bones was made (Robertson, 1967). The identities of the bones which were recovered from the red and pink siltstone were tentatively referred to genus *Massospondylus,* and the red beds, which were later described as the Mpandi Formation hosting the reptilian bones (Thompson, 1975). The first occurrence in Zimbabwe of the now invalid taxon *Euskelosaurus*, was reported from the Sentinel Ranch in the Tuli Basin. The fossil bones were recovered from the lower exposures of the Mpandi Formation, and this was postulated to correlate with the occurrence of the same taxon in the Elliot Formation of the main Karoo Basin of South Africa (Cooper, 1967). Further historical research activities on vertebrate palaeontology in the Tuli Basin were also at the Sentinel Ranch, where the presence of the two previously identified genera was reported. An almost complete in-situ *Massospondylus* skeleton was reported from an outcrop in the same ranch (Munyikwa, 1997, Rogers *et al*., 2004).

Most of the fossils from these beds exhibit haematitic red colouring, suggesting deposition in oxidizing environments (Bordy and Catuneanu, 2001). These strata also exhibit very faint bedding as shown in Figure 1.4a. During a previous study (Zondo, 2019), fossil bones collected over the last decade and those historically collected from Sentinel Ranch were identified. Whereas historically, authors considered the dinosaur fossils to pertain only to the sauropodomorph genera *Massospondylus* and *Euskelosaurus* (Thompson, 1975). The study identified a diversity of genera, including *Massospondylus, Melanorosaurus*, *Sefapanosaurus* and *Pulanesaura* dinosaurs (Zondo, 2019). These taxa have a co-occurance in the Elliot Formation and help to tentatively correlate the Mpandi Formation to the Elliot Formation. The genus "*Euskelosaurus*" has since been invalidated as a taxon (McPhee *et al*, 2017). This meant there was need to work on the correlation of the Mpandi Formation, using current information.

Sauropodomorphs had a broad distribution in the Mesozoic which makes them global biostratigraphic indicators for periods from the late Triassic to Early Jurassic (McPhee *et al*., 2017). In the Main Karoo Basin, occurrences of sauropodomorphs were formerly divided into two biozones, the "*Euskelosaurus"* and the *Massospondylus* range zones, which have been revised by Viglietti *et al,* (2020a, b), to the *Scalenodontoides* and *Massospondylus* Assemblage Zones, respectively (SAZ and MAZ). The former is entirely within lower Elliot Formation and Late Triassic in age, and the latter in the upper Elliot to the Clarens Formation. The index taxa in the SAZ are the traversodontid cynodont, *Scalenodontoides*, found together with sauropodomorphs, like *Blikanasaurus* and *Melanorosaurus*. Other sauropodomorphs found exclusively in the SAZ include *Plateosauravus*, *Eucnemesaurus*, *Kholumolumo*, *Sefapanosaurus*, and *Meroktenos*. The MAZ has the following taxa: *Massospondylus*, *Arcusaurus*, *Ignavusaurus*, *Aardonyx* and *Pulanesaura* (McPhee *et al*., 2017; Bordy, 2020; Viglietti *et al,* 2020 a, b). In the MAZ the main index taxa is *Massospondylus*, together with the *Lesothosaurus* and the *Protosuchus*. The co-occurrence in the Mpandi Formation of some taxa from the lower and upper Elliot, and the Clarens formations, is vital for correlation of the beds. This suggested that the Mpandi Formation may extend across a much greater time span than previously thought and includes a much more diverse ecosystem.

Table 1.1 Lithostratigraphic schemes for the main Karoo Basin, the Tuli Basin of South Africa, Tuli Basin of Botswana and the Tuli Basin of Zimbabwe (modified after Rogers *et al*., 2004).

Karoo Basin (main) (Johnson, 1994)		Tuli Basin South Africa (Bordy and Catuneanu, 2001, 2002a)	Tuli Basin Zimbabwe (Thompson, 1975)	Tuli Basin Zimbabwe (Cooper, 1980)	Tuli Basin Botswana (Smith, 1984)	
Stormberg Group	Clarens Formation	Clarens Formation	Forest Sandstone	Samkoto Formation	Lebung Group	Tsheung Sandstne Formation
						Thune Formation
	Elliot Formation	Upper Unit	Red Beds	Mpandi Formation		Korebo Formation
	Molteno Formation	Middle Unit	Escarpent Grit	Gushu Formation		
Beaufort Group		Middle Unit				
Ecca Group		Basal Unit (undifferentiated)	Fulton's Drift Mudstones	Fulton's Drift Formation	Seswe Formation	
					Mofdiahogolo Formation	
Dwyka Group			Basal Beds (undifferentiated)	Dwyka diamictite		

The Mpandi Formation is capped by a pedogenic silcrete separating it from the overlying Forest Sandstone Formation (Munyikwa,1997; Bordy, 2000; Bordy and Catuneanu, 2001; Rogers *et al.,* 2004). This layer is a convenient indicator facies across the basin. The occurrence of the silcrete is indicative of a long period of non-deposition and lack of erosion at the close of the Mpandi Formation (Rogers *et al*., 2004). Silcretes form through precipitation of silica from saturated ground water, and recrystallisation episodes (McCoy, 2011;Thiry and Milnes, 2016).

The Forest Sandstone Formation comprises light brown, fine- to- medium grained aeolian sandstones (Figure 1.4b). The sandstones are quartz-rich and well sorted

(Bordy, 2000; Rogers *et al*., 2004). It also shows some faint large-scale crossbedding most likely of aeolian deposition. The Forest Sandstone Formation exhibits chert clasts on its basal portion, eroded from the Mpandi silcrete. This formation has an estimated exposed thickness of about 20m while on the South African side, its equivalent unit, the Clarens Formation, is said to reach an exposed maximum thickness of 45 – 50m (Bordy and Catuneanu, 2002; Rogers *et al*., 2004). No fossils have been recovered from this unit on the Zimbabwean portion whilst several trace fossils, *Massospondylus* and *Syntarsus* tracks have been found in the Clarens Formation on the South African side of the Tuli Basin. *Massospondylus* bones have been found implying that its age is early Jurassic (Bordy, 2000; Bordy and Catuneanu, 2002). The Forest Sandstone Formation sandstones are contact metamorphosed from overlying basaltic lava (Bordy, 2000). The close of the episode of sediment deposition in the Tuli Basin, like in the main Karoo Basin, is marked by the emplacement of igneous rocks from the eruption of magma (Munyikwa,1997; Bordy, 2000; Bordy and Catuneanu, 2001; Rogers *et al*., 2004). The eruption of Tuli Basalts preceded that of the Large Igneous Province in the main Karoo Basin. According to a study by Rogers et al (2004), the Tuli Basalts are dated at around 186 ± 1.2 Ma while the Karoo Basin eruptions occurred around 183 Ma (Rogers *et al*., 2004; Linol *et al*., 2016).

Table 1.2. Lithofacies of the Tuli Basin (Rogers et al, 2004).

Formation	Lithology	colour	Sedimentary structures	Fossils	Interpretation
Forest Sandstone	Quartz rich fine to medium grained sandstones	Pinkish white to brownish (yellow)	Tabular & trough cross- bedding, Faint large-scale cross- bedding	Not known	Aeolian deposits
Mpandi	Quartz rich sandstones, siltstones, silty claystones	Red, purple to light grey	Silicified root traces, carbonate nodules, trough cross-bedding	Vertebrate	Over-bank deposits in semi-arid environments
Gushu	Conglomerate, Upward-fining Coarse to very coarse sandstones	White to pale-grey or pink	Interbedding & cross- bedding	Not known	Fluvial deposits
Fulton's Drift	Argillaceous shales, mudstones, coal seams, sandstones	Grey to black	No structures	Plant impressions	Deposited in shallow, stagnant basin in tundra environments
Dwyka	Conglo-breccias	Grey to black	No structures	Not known	Deposited in cold, fluvial- lacustrine environments

The Tuli Basin lower Karoo strata are not exposed within the study area, but briefly described below commencing with the basal beds.The Dwyka Diamictite Formation is also referred to as Basal beds (Robertson, 1967; Thompson, 1975; Bordy, 2001). Dwyka-type formations across the Karoo-related systems in all Gondwana continents began in late Carboniferous to approximately end- Carboniferous or Early Permian (Smith, 1990). The beds comprise polymictic-conglo-breccias, angular and subangular unsorted fragments of basement rocks, bound by argillaceous matrix. The Dwyka beds are characterized by structureless, poorly-sorted conglomerates, sandstones, and a few mudstones horizons. The formation is approximately 25m thick (Bordy, 2001, Rogers *et al*., 2004), and was deposited in glacial environments (Mennell, 1905), when the direction of flow was from ENE to WSW (Bordy, 2001).

The Fulton's Drift Formation comprises argillaceous shales, mudstones, coal seams and occasionally a few white to light grey lenticular sandstones. In lower parts of the formation, pebble beds are also present. The contact with the overlying Gushu Formation is marked by a thin layer of conglomerate with rounded pebbles including silicified wood and chert, with fossil plants. The beds were deposited in Tundra environments. Fulton's Drift corresponds to the coal-bearing Ecca Group in the main Karoo Basin and Tuli Basin South African side (Rogers *et al*, 2004; Bordy, 2001).

The Gushu Formation measuring a thickness of up-to 15m overlies the Fulton's Drift Formation. The upward-fining coarse to very coarse sandstone facies are occasionally interbedded and cross-bedded. The beds are white to pale grey or pink in colour. The Gushu Formation usually exhibits beds of small, angular-to-subangular pebbles. The Gushu is correlated to the Escarpment Grit in the Zambezi Basin and Molteno Formation in the main Karoo Basin. The correlation is based on lithological evidence due to lack of fossil remains in Gushu Formation (Rogers *et al*, 2004; Bordy & Catuneanu, 2002; Bordy, 2000). It marks the base of the Upper Karoo Group in Zimbabwe.

Unlike similar localities in the main Karoo Basin of South Africa, the palaeontology of the Tuli Basin portion in Zimbabwe has been poorly studied, with only two publications dedicated to this subject in the last 30 years (Rogers et, 2004., Thompson, 1975).

Figure 1.2. Google Earth map screenshot of the Sentinel Ranch new fossil sites at the Wedding Hill, Pimwe and old Homestead, depicted by orange dots.

For this project I continued collecting fossils I identified in the field and revisited the new fossil sites I discovered to collect sedimentological and stratigraphic data to test against the Rogers *et al*. (2004) framework.

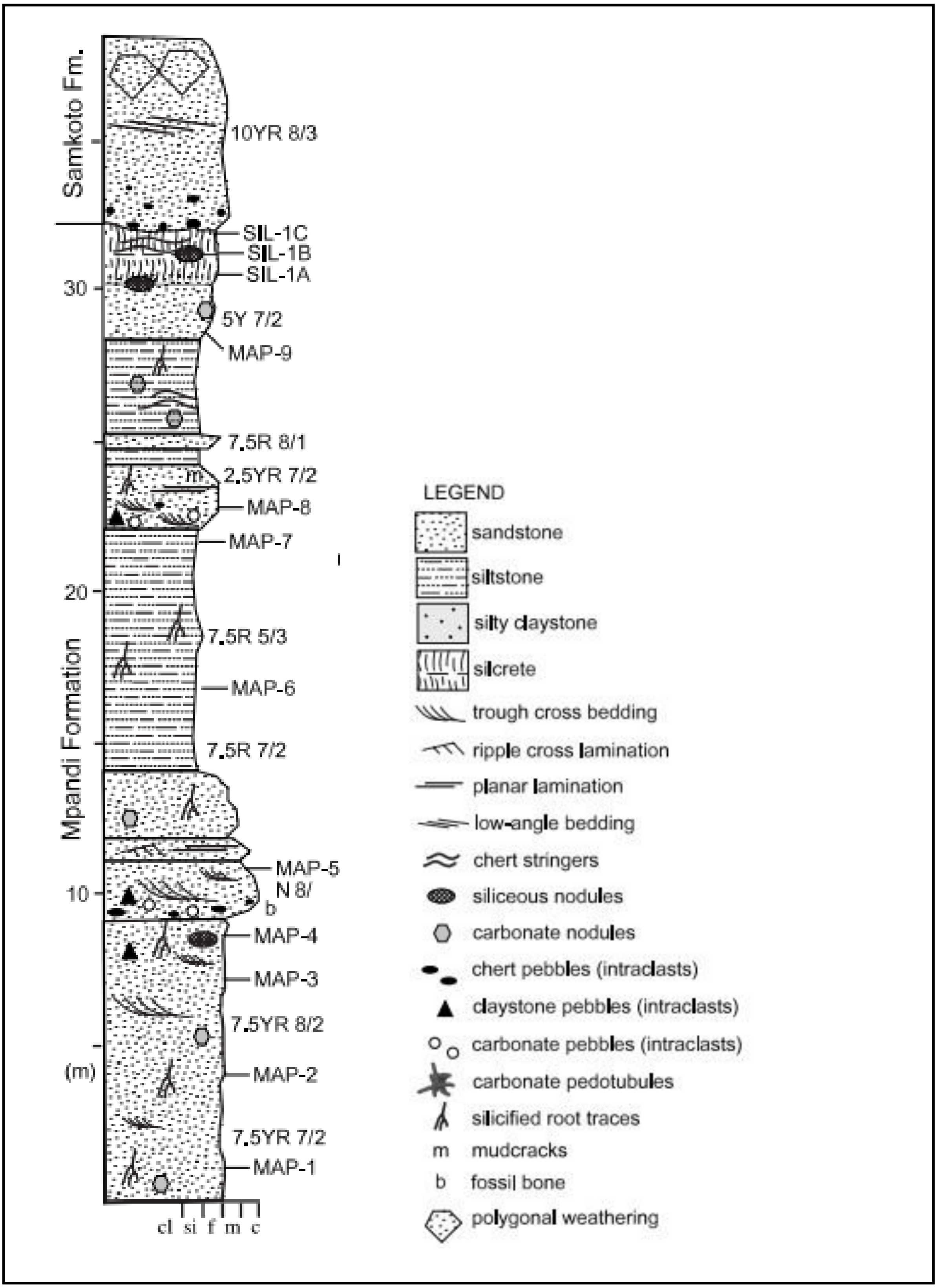

Figure 1.3. Generalised lithostratigraphic scheme of the Tuli Basin at Sentinel Ranch (modified after Rogers et al, 2004).

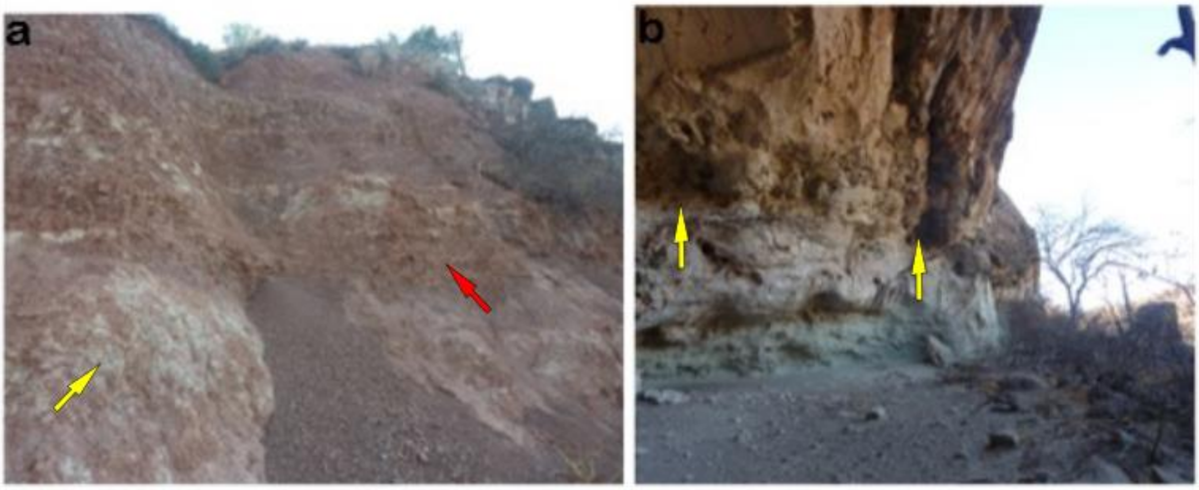

Figure 1.4. (a). The Mpandi Formation beds at the Limpopo Riverbed, at the old homestead site. It exhibits faint trough cross bedding shown by a red arrow midway to the top; the lower part shows mottling shown by a yellow arrow. (b). The upper stratigraphical region of Mpandi Formation where it contacts the light brown sandstones of the Forest Sandstone Formation.

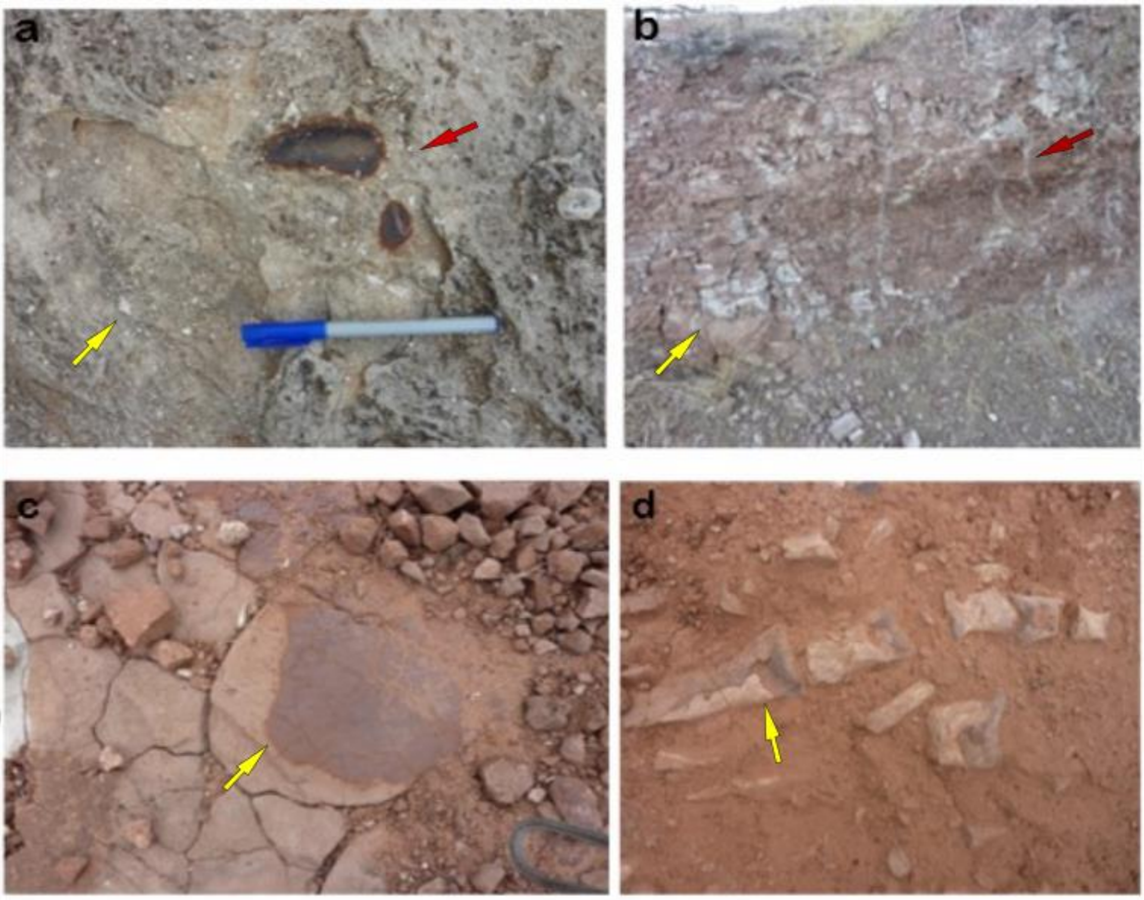

Figure 1.5. (a), Grey fine sandstone with carbonate nodules and haematite-rich teeth encasings, (b), Mpandi purple mudstones exhibiting blocky weathering with vertical and subvertical root casts. (c), fine-grained light brown sandstone with red patches indicating oxidation effects. (d), coarse-grained sandstone with gravel clasts, it also shows dinosaur foot bones.

Sedimentation

The main Karoo Basin formed in response to tectonic subduction and orogen processes on the southern margin of the Gondwana (Catuneanu, 2005). whereas the Tuli Basin and the other basins to the north of the MKB formed through extensional or trans-tensional forces that spread towards south from the divergent Tethyan margin of Gondwana into the super continent. (Catuneanu, 2005; Watkeys and,Sweeney,88).
The sedimentation in the main Karoo Basin and the related similar aged basins in the south-to-central Africa generally commenced around the Late Carboniferous period (~300 Ma) and abruptly terminated with the extrusion of basaltic lava in the Lower Jurassic interval (around 183 Ma), though with an earlier eruption at around 186. 3 Ma in the Tuli Basin (Catuneanu *et al*., 2005, Rogers *et al*., 2004). The sequence in the Tuli Basin was deposited on a highly metamorphosed gneiss rocks (Robertson, 1967; Thompson, 1975).

The historical search for coal in the Tuli Basin contributed to the gradual growth of knowledge of the Karoo sediments in this basin. As early as 1905, there were some investigations into the presence of some MKB equivalent beds in the Tuli Basin which led to the discovery of Dwyka beds that were thought to be absent in the sequence (Mennell, 1905). Several researchers had recognized the presence of Karoo sequences that sit on basal gneiss rocks and had also noted that the sedimentary sequence was capped by basalt rocks. Descriptive names were given to the formations based on the sedimentology of the beds, but different prospectors gave different names over time. Plant leaves impressions were found to be present in the Fulton's Drift Formation while fossil bones were recovered from the red beds. The fossil vertebrate bearing beds were at some time called the Siltstone Formation (Robertson, 1967) and they were latter referred to as the red beds (Thompson, 1975). Correlating the sediments within the basin, and with beds from the neighbouring and regional basins always presented challenges because the strata are narrow and less continuous contrary to the situation at the MKB where beds can occupy hundreds of metres in thickness exposures (Robertson, 1967); Thompson, 1975; Much of the information of the buried strata was made available through historic borehole logs produced during the prospecting for economic minerals such as coal (Thompson, 1975). On the South African side of the Tuli Basin, comprehensive studies have been conducted in recent times where the lithology, stratigraphy and sedimentation of the beds were described. The Tuli Basin beds were found to comprise sandstone facies assemblages, fine grained facies assemblages, gravel facies assemblages, where direction of flow was not always constant over time (Bordy, 2000; Bordy and Catuneanu, 2001, 2002,). The capping basalts were also split into stratigraphic sequence with olivine basalts at the lower sections and the upper parts being augite-plagioclase-phyric basalts (Vail *et al,* 1969).

Dating and Correlation

In historical palaeontological studies of the Tuli Basin, the Karoo beds have been said to be equivalent to the beds of the main Karoo Basin based on lithology and biostratigraphic comparisons. The basal Dwyka diamictite beds have been correlated to the Dwyka Formation beds of the MKB based on the similarities of lithologies and their basal stratigraphic positions (Thompson, 1975; Catuneanu et al.). The superimposed Fulton’s Drift Formation is equivalent to the Ecca Group in the MKB, and they are both characterised by similar lithologies, occurrence of coal seams and the presence of fossilised plant material (Robertson, 1965; Bordy, 2000). Gushu, the succeeding formation, is postulated to be equivalent to the Molteno Formation of the Stormberg Group based on lithological grounds because of lack of fossils in the Gushu Formation (Thompson, 1975; Bordy, 2000). The overlying vertebrate fossil-bearing Mpandi Formation has been correlated to the Elliot Formation. The taxa with co-occurrence in the MKB that were used in historical biostratigraphy of the Mpandi Formation in the Tuli Basin is the *Massospondylus* and the *Euskelosaurus* dinosaurs, but the latter genus is now a nomen dubium. This has left the determinations based on this taxon questionable and requiring revision because of the invalidation of the *Euskelosaurus*. The succeeding Forest Sandstone Formation is the equivalent of the Clarens Formation in the MKB, and the corelations are also based on lithological grounds due to lack of fossils in the former (Thompson, 1975). A radiometric analysis method was employed at the Tuli Basin nearly two decades ago, when the age of the Tuli basalts overlying the Forest Sandstone formation, was estimated using the Potassium-Argon dating method (Rogers et al, 2004), providing an upper age limit for the Forest Sandstone Formation, which overlies the Mpandi Formation, of 186.3 ± 1.2 Ma.

CHAPTER 2

Methodology and Materials

Fieldwork

To assess the provenance of all collected specimens, two weeks of fieldwork was conducted at Sentinel Ranch between 2021 and 2022. A GPS was used to record the exact location of the fossil sites, geological features and sedimentary structures. It was also used to record the locations of points during the measuring of lithostratigraphic sections.

Stratigraphic sections were measured using an Abney level, Jacob's staff, GPS units, etc. In determining the thickness of the stratigraphic section, an Abney level or a Jacob staff was used to make measurements. A GPS unit was used to record the track of measured sections and coordinates of each measurement of the stratigraphic section. The schemes set out by Miall (1996), and Rogers *et al* (2004) were employed when characterizing the rock facies and field observations of features such as colour, grain size, and sedimentary structures.

Fossil identification

To identify the fossils collected during the fieldwork, they had to be first cleaned of matrix using air scribes and then all the features and characters including morphology of the fossils were observed. The fossils were then classified to their precise lowest possible taxonomic group by comparing the defining features of the fossils with those of similar fully described specimens or holotypes. Major research collections institutions such as the Natural History Museum of

Zimbabwe and the Evolutionary Studies Institute (ESI), at Wits University were consulted for comparisons. The stratigraphic occurrence of taxa in the Mpandi Formation were noted and correlated to the occurrence of similar taxa at the MKB.

Age assessment

Biostratigraphic divisions set out in (Viglietti *et a*l, 2020a, b; Bordy *et al* 2020; McPhee *et al* 2017; Kitching, and Raath 1984) were used in determining the relative age of the Mpandi sediments.

To conduct detrital zircon dating of the Mpandi Sediments, rock samples from the formation were collected from 3 different fossil sites at different stratighical levels from bottom to top of the sections.. The rock samples were crushed to separate minerals at the University of Johannesburg.

About 100 to 150 zircon grains were selected and strictly not less than 60 grains, in this case random and non-random grain selection protocol was employed (Anderson, 2005).

Before the selection was done, all grain sizes, morphologies and colour were identified by visual inspection and purposely selected several grains of each kind (that is random selection). Then at the end of grain selection session, a few randomly selected grains were added to the mix.

Mounted zircons were shipped to the Imaging and Analysis Centre at the Natural History Museum of London (UK) for age assessment using standard LA-ICPMS techniques. An Agilant 8900 quadrupole ICP-MS coupled to a Teledyne Iridia 193 nm excimer laser. The laser was operated at 8 Hz repetition rate, with a fluence of 2.5 J cm-2 and a spot size of 25 µm. GJ-1 (ca. 601 Ma; Jackson et al. 2004) was used as the primary geochronology standard and Plesovice and zircon 91500 were analysed between each set of unknowns to ensure consistency and accuracy in the U–Pb ages obtained (Wiedenbeck et al. 2004; Sláma et al. 2008) Data reduction was performed using Iolite v.3.61 (Paton et al, 2011). Downhole fractionation corrections on the $^{206}Pb/^{238}U$ and $^{207}Pb/^{235}U$ ratios were conducted using VisualAge. Analysis that were found to be discordant or having excessive La contents are not reported in the reported data. The results were analysed and interpreted using the approach of determining maximum depositional ages as laid out in Bordy *et al* (2020).

Paleoenvironments

For the reconstruction of paleoenvironments and paleoecology, biostratigraphic and lithostratigraphic information was used. Biostratigraphic information was used to infer the paleo-biodiversity and information from sedimentary structures, facies, and taphonomy of the fossils to infer the paleoenvironments. If the fossils were articulated and in early weathering stages, it would be inferred that the animals were buried not far from their death place and that they did not remain for very long periods of time in subaerial environments on the floodplains before burial. This would suggest frequent sedimentation events such as flash floods. If they were widely scattered, isolated, and disarticulated, it would be inferred that the carcases were exposed for much longer times after death before burial and, also infer that there was infrequency of sedimentation events such as in semi-arid environments.

Miall (1996) facies codes for sedimentary rock facies was adapted and used in this study for description of the sedimentary rocks based on their depositional environments and characteristics as detailed below.

Table 2.1. Identified lithofacies. Lithofacies code is slightly modified after Miall (1996). Sedimentary structures observed within the study area.

Lithofacies	**Lithofacies code**	**Sedimentary structures**	**Interpretation**
Conglomerate, massive or bedded clast supported	Gcm	Massive or faintly bedded	Pseudo debris plastic-flow
Sand, fine to coarse	St	Trough cross-lamination	Migrating dunes
Sand, Fine to coarse	Sp	Planer cross-lamination	Lingoid bars (lower flow regime}
Sand, very fine to coarse	Sr	Ripple marks	Ripples (lower flow regime)
Sand, fine to coarse	Sm	Massive or feint lamination	Rapid deposition
Sand, very fine to very coarse	Sh	Bedding- parallel lamination	Plane bed flow (low and high flow regime)
Sand, fine to coarse	Ss	Boad shallow scours	Scour fills
Sand, very fine to fine, silt, mud.	Fm	Massive to laminated	Waning flow deposits
Sand, very fine to fine, silt	Fl	Fine lamination, small ripples	Waning flow deposits

CHAPTER 3

Facies descriptions, Sedimentary structures, and stratigraphic Sections

In this project two stratigraphic sections were measured at the sites “Wedding Hill” and “Pimwe Hill”, and detailed logs were developed. There were important vertebrate fossils discoveries at these sites which have brought new knowledge and understanding about fauna at the Sentinel Ranch. These and other fossil sites at the Sentinel Ranch are shown in Figure. 3.1. The new discoveries at these sites rendered it necessary to have detailed sections of the outcrops.

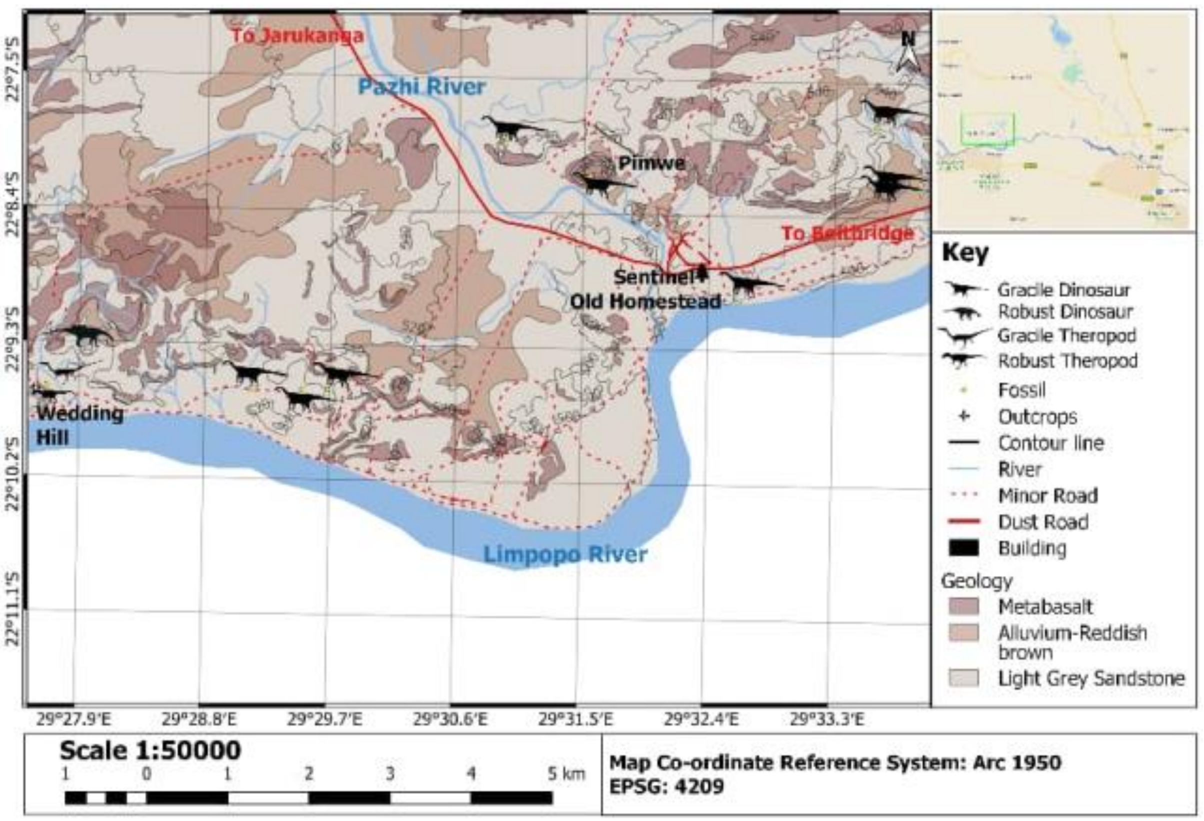

Figure. 3.1: This figure shows the locations of the sites “Wedding Hill” and “Pimwe Hill” on the Sentinel map. It also shows the depictions of taxa found in respective sites.

The Wedding Hill

The outcrop is situated to the west of the homestead just across the Sizi River. It represents the upper sections of the Mpandi Formation. At the base of the hill where the logging started, the GPS position reading was 022, 163875^0 S: 029,46198^0 E. This outcrop has a logged height of 14 metres from the base to the silcrete (Figure. 3.2). Massive brown fine-grained sandstones characterise the basal sections of the Hill. These brown sandstones are overlain by a silty fossiliferous purple bed. The stratum is a fossil bed that produced many post-cranial bones of both the small-sized and medium-sized theropods, there were also small-sized, medium-sized and robust sauropodomorphs on the bonebed.

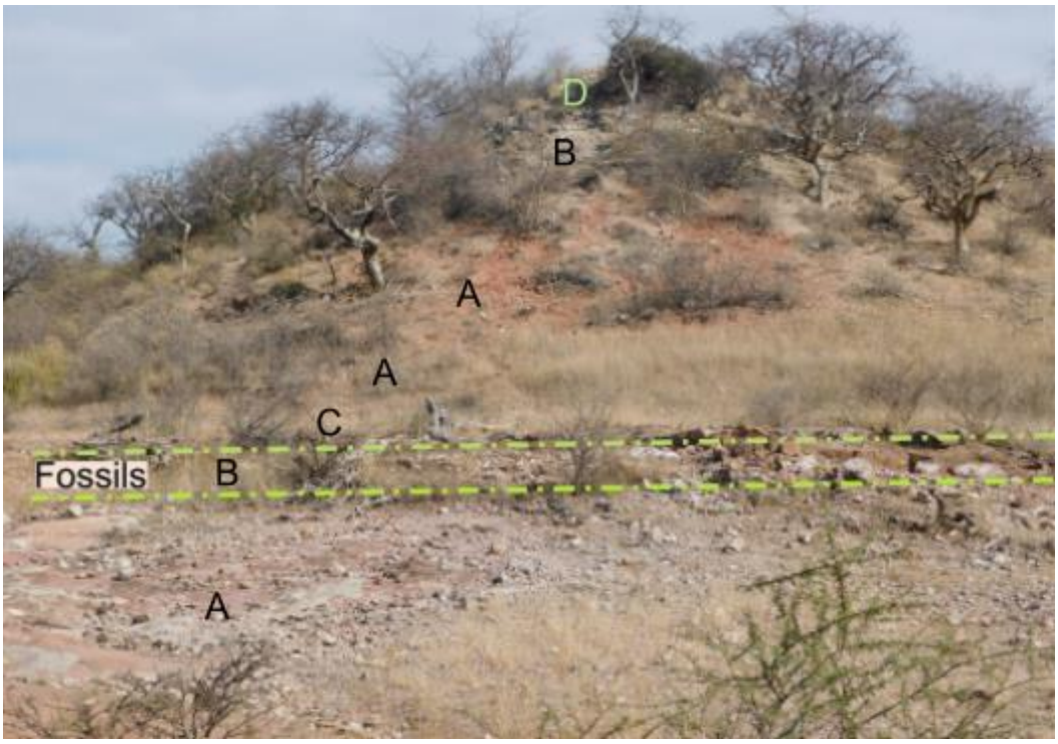

Figure. 3.2: The Wedding Hill, the yellow lines indicate the bonebed from where the fossils were collected. The alphabetical letters represent the lithofacies as seen on the outcrop.

The purple bone-bed is overlain by a light-grey conglomerate bed which has a thickness of about 0.60 m. The conglomerate bed is overlain by massive red brown sandstone strata that spots some pedogenic concretions. On the upper sections of the outcrop, the beds are grey-coloured plane-bedded siltstone. This bed culminates into a silcrete which is an erosional surface where the upper sections have been lost to erosion, the bed can be traced laterally in the study area on many outcrops. Typically, the silcrete is overlain by the Forest Sandstone beds in the area which are in-turn overlain by basalts, all of which are now missing on the outcrop due to erosion. Figure. 3.3. shows a detailed stratigraphic section of the Wedding Hill, and the lithofacies are described in the following sections.

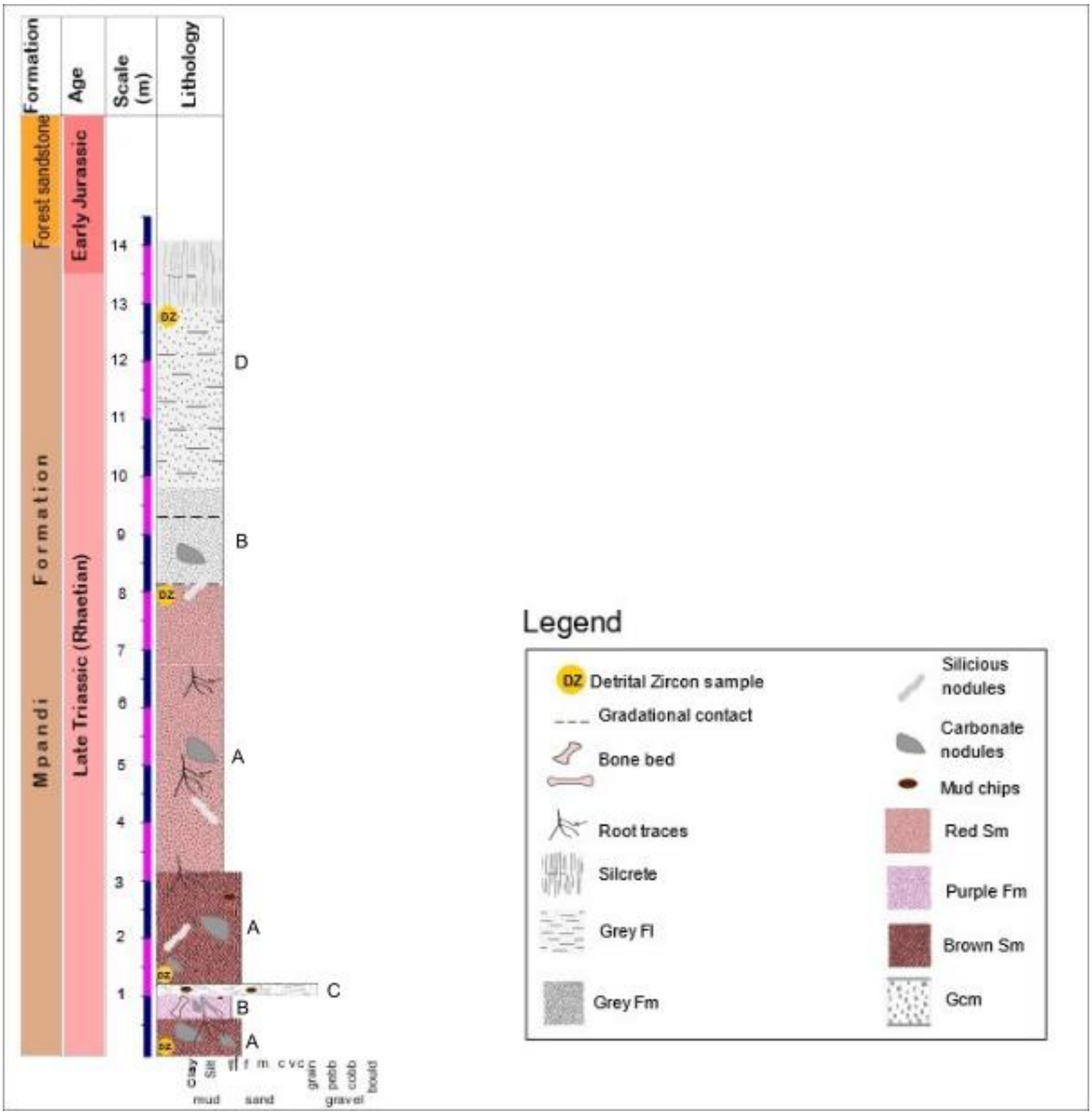

Figure 3.3. The stratigraphic section of the Wedding Hill at Sentinel Ranch.

The Wedding Hill lithostratigraphic section

N.B. Lithofacies codes used are explained in Figure 2.1.

Facies A, fine-grained sandstone, facies Sm

The logged section of the wedding Hill is completely contained within the Mpandi Formation as it ends on the silcrete. The unit is dominated by sandstone facies assemblages mainly represented by Sm and subordinate Gcm facies, and fine-grained assemblages, comprising Fm and Fl lithofacies. At the base of the section are brown Sm lithofacies that spot greyish irregular-shaped pedogenic carbonate concretions Figure 3.4. The concretions have a wide size range from about < 1cm to about > 1m. This fine-grained bed also shows some feint silicified root traces. There are mudstone clasts on the Sm beds. Fm, and a Gcm beds occur in-between this Sm bed and a similar bed that occurs overlying the Gcm lithofacies.

Figure 3.4. Sm stratum in the basal sections of the outcrop. This bed exhibits pedogenic concretions.

Facies B, fine-grained silt facies Fm.

Purple Fm beds overly the basal Sm beds. This stratum is a fossiliferous bonebed which also exhibits some carbonate nodules and feint silicified root traces. The bed is massive and shows no visible bedding lines. Theropod and sauropodomorph bones were recovered from this bed Figure 3.5. The fossils seem to be preserved in a silicious matrix which gives the bones a whitish outlook. Some silicious concretional structures are also present on this sediment.

Figure 3.5. Purple Fm lithofacies with sauropodomorph and theropod bones. The bed also exhibits some carbonate nodules.

Facies C, the conglomerate Gcm facies.

A Gcm bed overlies the bonebed and is overlain by the Sm bed. The Gcm is a clast-supported conglomerate sediment composed of silicious clasts, carbonate nodules, mudstone clasts, siltstone clasts, rounded bone fragments, and the clasts fine-upward. No fossils were found on the bed. Figure 3.6. Shows the Gcm bed. A red Sm bed, similar in composition to the already described, but differing in colour and in that it has a sporadic occurrence of small patches of mud drapes, overlies this conglomerate bed.

Figure 3.6. A Gcm bed, fining upward, the bed lies on the bonebed.

Facies D, the fine-grained assemblage Fm/Fl facies.

Fine-grained facies assemblage is also present at the upper sections of the outcrop. These are mainly represented by Fm and Fl lithofacies, which comprise siltstones and mudstones. This fine-grained lithofacies from about 8 metres below to the top of the section. Few pedogenic concretions can be spotted on these beds. These grey coloured Fl lithofacies culminate into silcrete.

The silcrete is a silicious bed that caps the Mpandi Formation and is laterally continuous on many outcrops in the study area. The silcrete shows an appearance that resembles breccia. No fossil bones were found on the silcrete horizon. Some very feint plane bedding can be seen on the silcrete. Figure 3.7 shows the silcrete horizon.

Figure 3.7. An erosional silcrete horizon at the Wedding Hill.

The Pimwe Hill

This outcrop is positioned to the north of the old homestead on the banks of the Phazhi River, on the close to the camp. The measured logged section on this outcrop is 60 metres high from base to the top of the basalt. The Pimwe Hill preserves the sequence from the upper Mpandi Formation, the overlying Forest Sandstone, and to the capping basalts.

The outcrop is made of sandstone facies assemblages comprising lithofacies Sm, Sh, Sl, Sp, St, sst, and the subordinate facies Gcm, and the fine-grained facies assemblages comprising the Fm and Fl lithofacies. Lithofacies Sm are the most dominant, followed by lithofacies Fm being second most common. The Sh lithofacies are the third most prevalent. The Sm beds show heavy bioturbation by invertebrates and some barrows can be associated with *Taenidium* sp.

An almost complete post cranial skeleton of a sauropodomorph dinosaur was discovered from the Pimwe Hill by the Bristows from a red bed about 7m uphill. Vertebrate fossils also occur on the upper sections of the hill, including on a Gcm lithofacies about 32m uphill above the base. The silcrete bed is present and is overlain by the Forest Sandstone stratum which is a fine-grained aeolian bed. The Karoo sequence is completed by the deposition of basaltic lava.

The Pimwe Hill lithostratigraphic section

N.B. Lithofacies codes are explained in Table. 2.1.

Facies A, Sandstones, facies Sm

The basal parts of the logged section at the Pimwe Hill comprise red Sm lithofacies with white patches at the bottom and Sh, St lithofacies below the middle sections to the top of the bed. The sediment has invertebrates' barrows that have been filled with red mudstone. This Sm and Sh bed occur in an alternating fashion with overlying Sc beds up to around 7m. Figure 3.8. shows this Sm/Sh sediment.

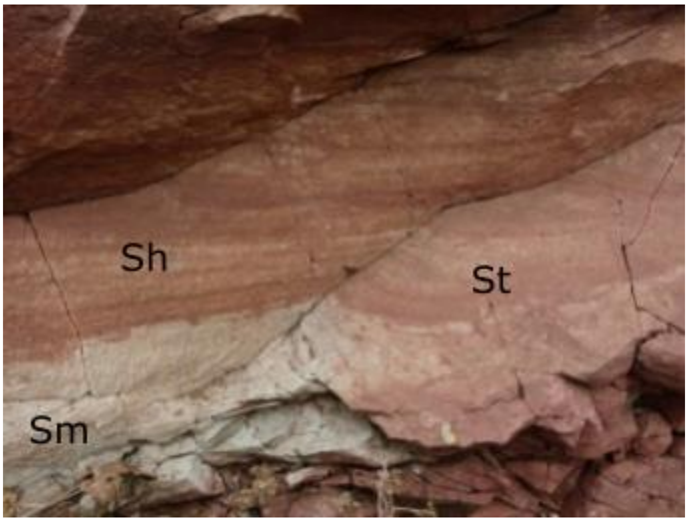

Figure 3.8. Sm/ Sh / St lithofacies at the basal sections of the Pimwe Hill logged section.

A heavily bioturbated massive sandstone Sm facies occur 3 metres up within the logged section. This very fine-grained bed on Figure 3.9.

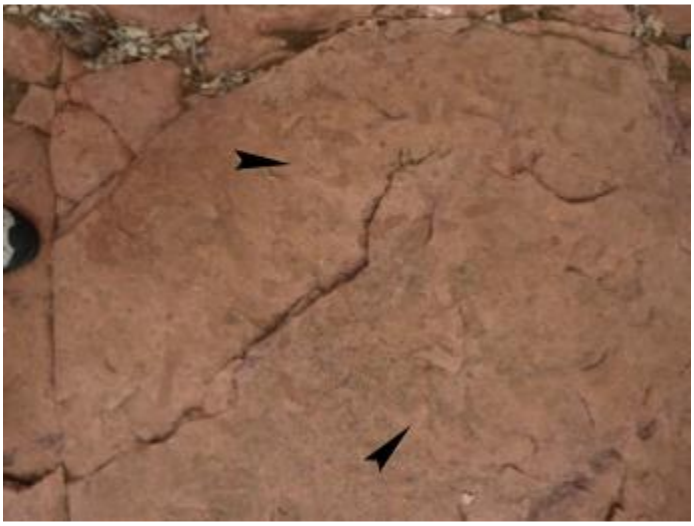

Figure 3.9. A heavily bioturbated Sm beds

Facies B, fine-grained facies Fm.

A red Fm bed is present, resting on the thin Sm bed overlying the Sc sediment. In this bed is where the almost complete postcranial skeleton of a medium-sized sauropodomorph dinosaur was found following a heavy rain. The sediment is a massive red mudstone, with sporadic occurrence of mud chips. The bed shows blocky weathering Figure 3.10.

Figure 3.10. An Fm lithofacies from where a sauropodomorph post cranial skeleton was recovered. The beds show blocky weathering.

Facies association A, sandstone, facies Sm

There are series of sediments of sandstone facies assemblages comprising Sh, Sm, Sp St, and fine- grained assemblage made of Fm, and Fl beds. At 12 m the stratum shows both the horizontal bedded and trough cross-bedded sandstones. The Sh bed displays small patches of mud drapes, Figure 3.11.

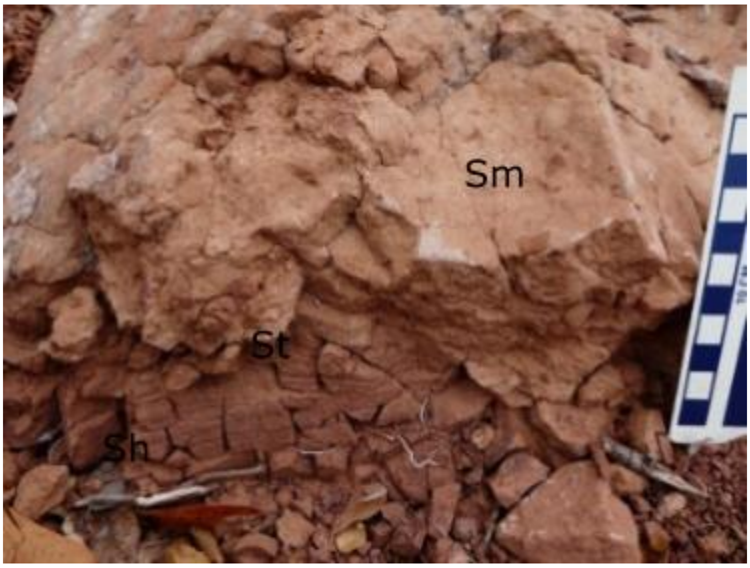

Figure 3.11. An Sh/St/Sm lithofacies showing plain, trough cross beds massive sandstone beds.

Facies D, the fine-grained assemblage Fm/Fl facies.

Fm/ Fl beds are present at around 12.3 metres up the stratigraphic section from the base. The beds are massive mudstones and siltstones occurring with horizontal bedded-mudstones and siltstones. Scour fills of sandstones and invertebrate burrows are also present in this sediment of red beds, burrows are filled with red siltstone/ mudstone. Carbonate nodules are present on the massive mudstones Figure 3.12.

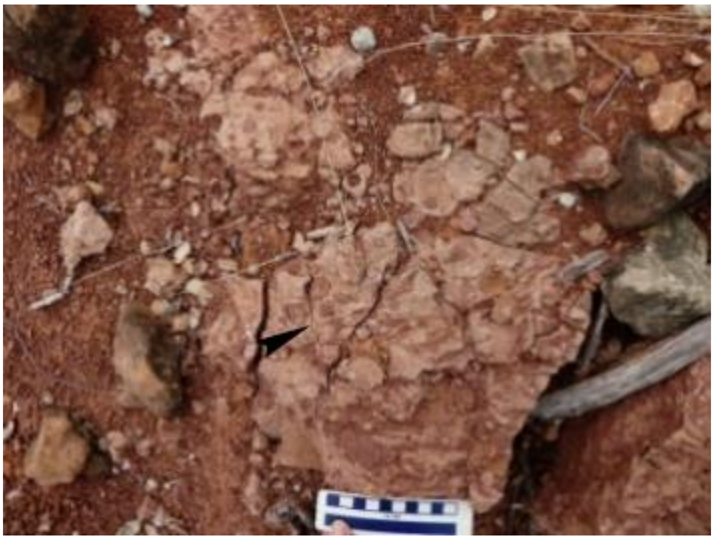

Figure 3.12. Fm/ Fl lithofacies displaying invertebrate burrows filled with red mudstone.

Facies A, Sandstone facies, facies Sm

Sm bed showing pebble lag at its basal sections. The pebble lag comprises mudstone clasts, siltstone clasts, carbonate nodules and silicious clasts in massive sandstone Figure 3.13 shows the Sm lithofacies with pebble lag. Fm beds rest unconformable on these Sm sediments and are interbedded by Sc and Sst sediments lying below the scree at 23 metres which obscures sediments.

Figure 3.13. A pebble lag on a Sm sediment showing clasts of mudstone, siltstone carbonate nodules on bottom part of sediment.

A matrix-supported very fine-grained Sst facies sediment with subangular clasts of mudstone, siltstone, sst and rare pedogenic nodules in Figure 3. 14.

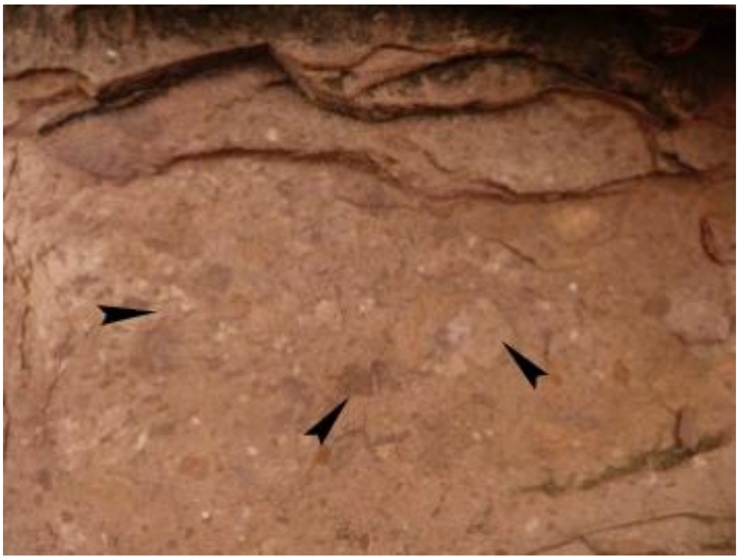

Figure 3.14. An Sst sediment showing clasts of mudstone, siltstone and pedogenic nodules.

Facies C, the infraformational conglomerate Gcm facies.

Some more beds are obscured by another scree of lose sediments lying above two strata of massive sandstones interbedded by a fossiliferous Gcm sediment. An in-situ fossil bone likely to be a limb bone of a medium sized animal was found sticking out on this breccia sediment. The bone is covered in haematitic matrix. The Gcm sediment is a clast supported bed with a silicious appearance, and bears some carbonate nodules, very fine Sst clasts, with angular and sub-angular clasts. Figure3.15.

Figure 3.15. A Gcm stratum displaying an unsorted arrangement of clasts. The bed is a clast-supported sediment.

Above the scree there is an Sm bed that culminates into a silcrete. The Sm bed bears silicious clasts and pebbles. The silcrete is a siliceous stratum with a breccia fabric, that seals the deposition of the Mpandi Formation. No fossils were observed on this sediment shown in Figure 3.16.

Figure 3.16. The silcrete is shown on the bottom part of the picture, displaying a Gcm breccia fabric. The arrow shows the contact of the Mpandi Formation and the Forest Sandstone Formation. The top part of the picture represents the lower sections of the Forest Sandstone with carbonate nodules and reap-up clasts from the underlying silcrete.

Forest Sandstone Formation beds are super positioned on the silcrete as shown on the Pimwe stratigraphic section Figure 3.17. The beds are light brown Sm facies. The bottom of the sediment is intercalated with rip-up clasts from the Mpandi silcrete. Fine- grained basalts cap the sedimentary rock succession at the Pimwe Hill. The Basalts are a brown coloured igneous rock but exhibit an olive-green colour when freshly weathered.

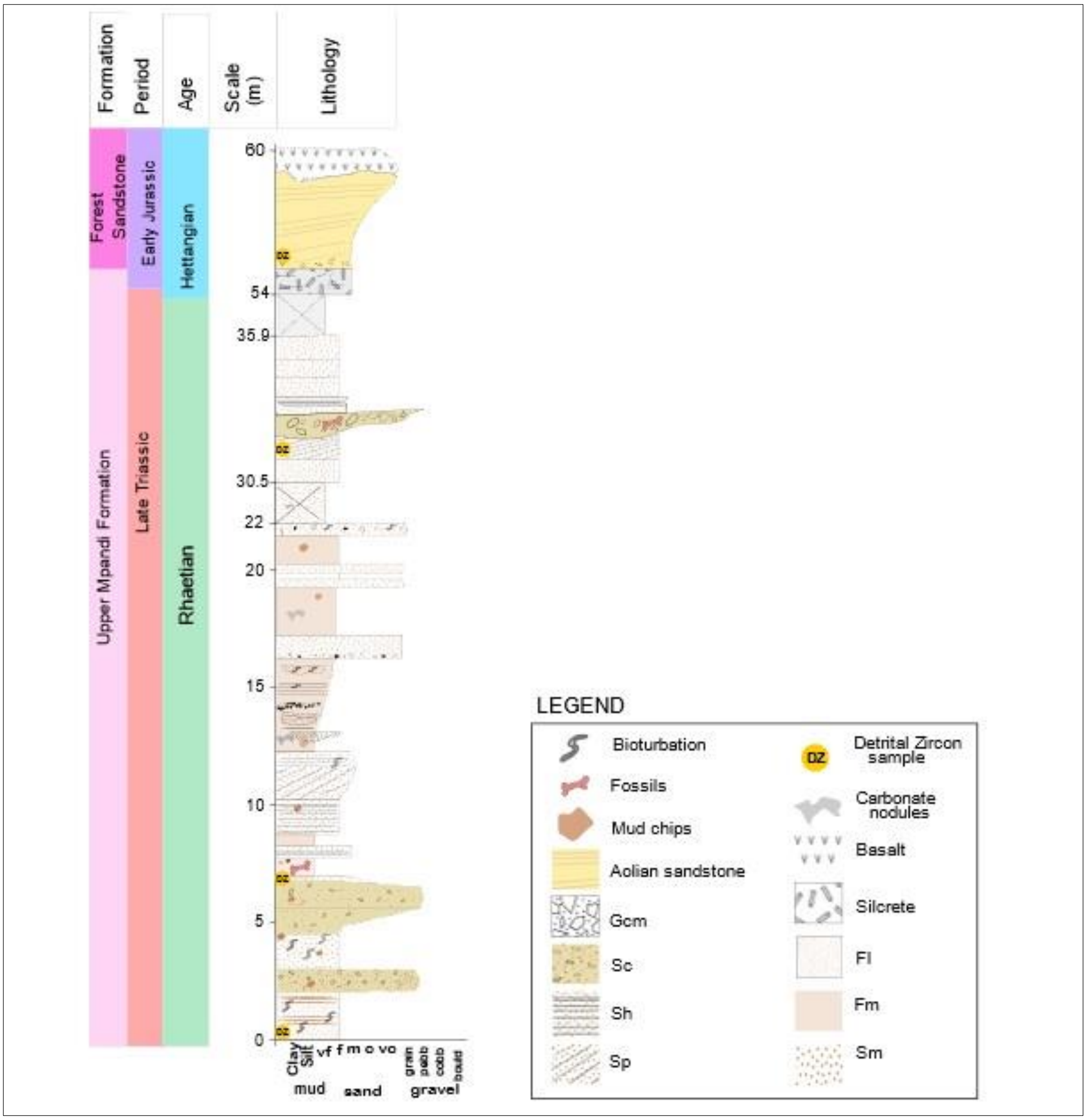

Figure 3.17. Pimwe lithographic section.

Sedimentary structures observed within the study area.

Bioturbation

Bioturbation traces by invertebrates were observed in various localities within the study area. Sm beds at basal portions of the Pimwe Hill exhibit heavy bioturbation with some showing distinct traces assignable to *Taenidium* isp. The traces are U shaped, oriented towards various directions. The bioturbation burrows exhibit different morphological designs likely to have been made by different insect species. Most burrows are tubular, vertical and sub-vertical insect borings. The burrows are filled with red mudstone, figure 3.18(A) shows bioturbation borings.

Roots traces

Root traces occur in some siltstones, mudstones, and fine sandstones in the Mpandi Formation. Roots traces represented by sub-vertical, squiggly and irregular lines of various sizes as well as colour mottling were observed at some sites (Rogers *et al*, 2004). Some root traces are shown in figure 3.18. (B).

Ripple marks.

Some ripple marks were observed in isolated slabs of beds at the ripple hill, showing an east to west direction of flow. The plan view of the ripples is sinuous, showing laminae with curvy up-and-down patterns, sometimes exhibiting cross-laminae. They dip in the direction of flow. Figure 3.18, (C) shows the ripple marks at the ripple hill.

Figure 3.*18*. (A) Invertebrate burrows of different morphology on a pinkish Sm lithofacies, (B) Shows root traces and mottling, (C) Ripples in fine-grained

sandstones, the direction of flow was east to west. The yellow dot indicates purple patches of mud rapes on the ripples.

The Sm lithofacies are the most common in the study area followed by the Fm lithofacies, and they usually occur in an alternating pattern as seen on figure 3.19.(A).

Calcareous vein

A calcareous vein was observed close to the bank of the Sizi River with a northwestern orientation, figure 3.19.(B). It appears as a white chalky vein cutting across the beds. It cuts through a light brown Sm bed, in a westward direction towards the Wedding Hill, which is close-by (Thompson, 1975).

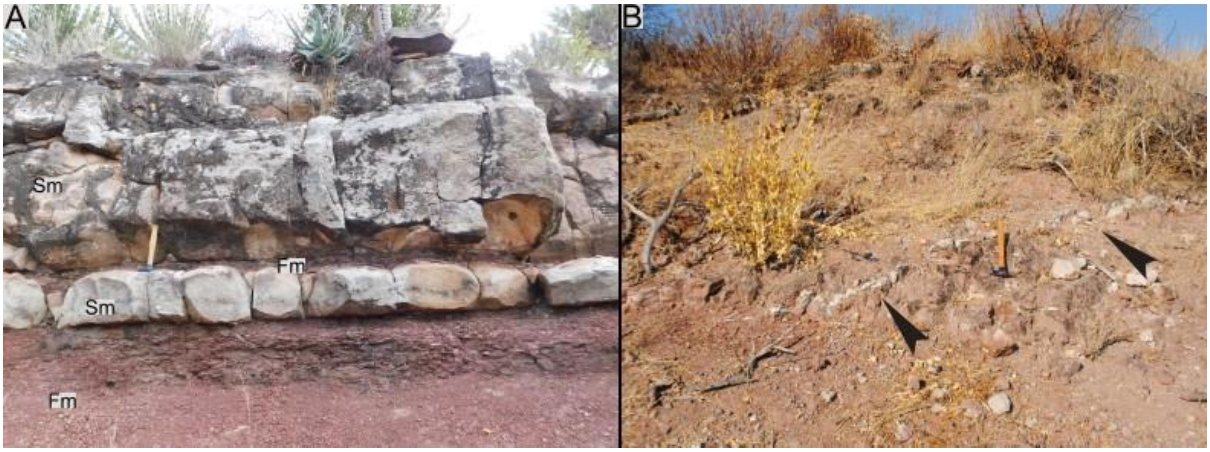

Figure 3.1*9*. (A) An Fm /Fl sediment occurring together with Sm beds in alternating patterns. (B) Shows a calcareous vein indicated by black arrows. The vein cuts across a brown Sm sediment.

Mud drapes.

Within the study area, in the Mpandi Formation beds, the sporadic occurrence of mud drapes is not uncommon in lithofacies Fm to silty and fine sandstones (Bordy and Catuneanu, 2001). Mud drapes appear as patches of thin red or purple mudstone sheets strewn on some rock surfaces. Mud drapes are shown occurring in association with desiccation cracks on figure 3.20.(D).

Desiccation cracks

Desiccation cracks as shown in figure 3.20, (A) were observed on some of the Fm lithofacies. The plan view of the desiccation cracks shows irregular polygonal shapes. The crakes were filled with finer mudstone and siltstone, forming a network of polygonal ridges on some mudstones and siltstones.

Flame structures.

Flame structures were observed on Fm lithofacies on an outcrop of the Mpandi Formation, the flame structures are shown on figure 3.20, (B). The cross-section view shows flame-like appearance of deformation on bedding lines.

Planar cross-bedded lithofacies (Sp facies).

The low-angle planar cross bedded strata were observed occurring in very-fine-grained sandstone units at some localities in the study area. The bedding lines are often very feint as seen in figure 3.20.(C).

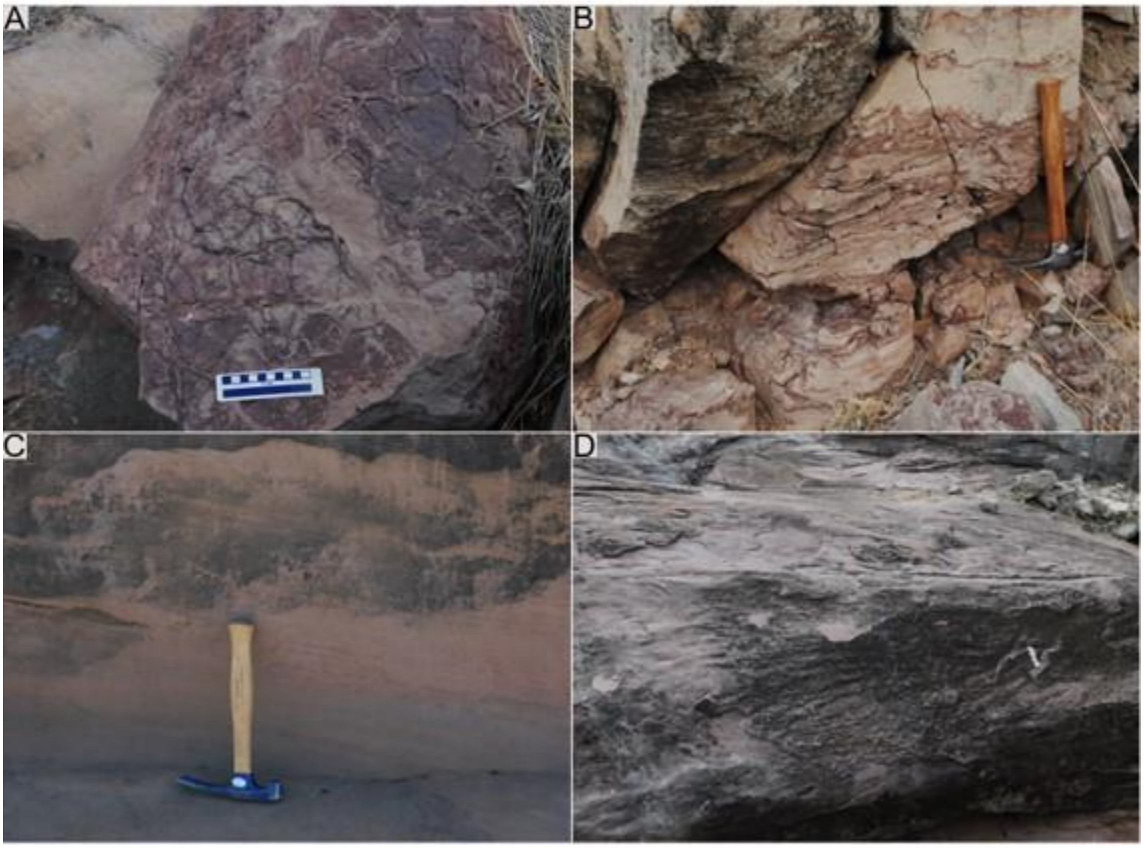

Figure 3.*20*. (A) Desiccation cracks on Sm lithofacies, (B) Flame structures in Fm lithofacies, (C) Sp lithofacies in fine sandstones. (D), St lithofacies on very fine-grained purple sandstone.

Trough cross-beds (St facies).

Trough-cross bedding was observed at a site where it occurs in very fine/silty purple sandstone, figure 3.20.(D). The bedding lines are low angled and extend to about the mid sections of the bed, the orientation is changed from there with the upper section forming a symmetrical appearance in relation to the bottom section.

Mud clasts.

Occurrence of mud clast is common in the study area and is observed occurring in association with the lithofacies Sst, Gcm, Sc, Sm and Fm at the Wedding Hill, Pimwe and other places. Figure 3.21 (A) shows some mud clasts exhibited on the Fm lithofacies.

Carbonate nodules.

The lower parts of the Wedding and the Pimwe hills exhibit some carbonate nodules, with the former showing some large blebby grey patches of limestone as shown on figure 3. 21(B). The carbonate nodules are a common feature in the Mpandi formation beds and the basal parts of the super adjacent Forest Sandstone.

Silcrete

The overlying Forest Sandstone Formation exhibit chert clasts eroded from the underlying silcrete, figure 3.21(C) (Rogers *et al*, 2004; Terry *et al*, 2001). It has breccia appearance because of silicified clasts and carbonate concretions, in fine matrix.

Silicious boxwork

Figure 3. 21(D), shows the complicated boxwork and or as long silicious veins commonly occurring in the Forest Sandstone rocks. The boxwork form weathering resistant ridges on the sandstones, creating networks of decorative silicified veinlets (Robertson, 1967).

Figure 3.21. (A) Fm facies sediment showing mud clasts and concretional material at the old homestead Limpopo Riverbank. (B) Carbonate nodules displaying subcircular structures on Sm beds. (C) A silcrete bed at Pimwe Hill with a breccia appearance (D) A Forest Sandstone bed exhibiting complicated silicious boxwork.

CHAPTER 4

Fossils

In this chapter fossils are described and identified to their lowest classification level possible using characters present in them and comparisons with already known specimens. The aim was to use the fossils for biostratigraphic age determination of the sediments.

Theropods have previously been found in the Mid-Zambezi Basin, Zambezi Basin, and the Carbora Basa Basin in Zimbabwe with the most prominent being the *Megapnosaurus* (*Syntarsus rhodesiensis*).

On this study, several fossil bones were found around the farm as indicated on the map, but of note was a bonebed at the Wedding hill. The bonebed produced small, medium sized and robust sauropodomorphs, as well as both small sized and medium sized theropod dinosaur bones. Figure 4.1. shows some of the important sites at Sentinel Ranch.

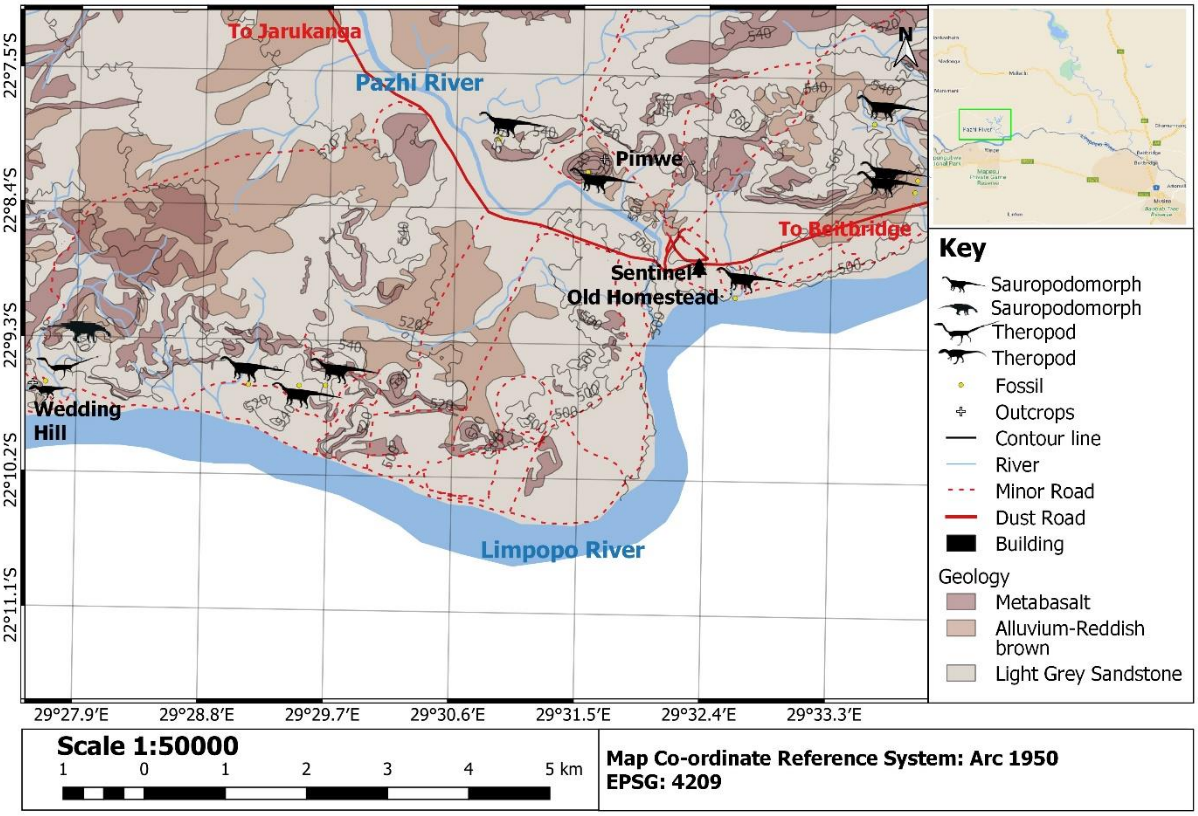

Figure 4.1. The diagram shows important fossil sites at the Tuli Basin, Zimbabwean side. The fossil sites are depicted by dinosaur images representing the suborder found at each site.

Many postcranial bones were collected from the bonebed at Wedding Hill fossil site. The bonebed occurs on fine-grained Fm lithofacies that have carbonate nodules and some irregular-shaped concretions. This bed is overlain by a conglomerate stratum which also have small bone chips likely derived from the bonebed. Among the bones discovered on the bonebed were limb bones of a robust sauropodomorph, comprising an articulated but heavily weathered tibia, fibula, phalanges and an ungual. These limb bones are displayed on figure 4.2.

Taphonomy of the bones collected from the Wedding Hill bonebed.

Some of the fossil bones collected from the Wedding Hill bonebed show sun cracking on the surfaces. Only the tibia, fibular and the foot bones were found in articulation, otherwise the rest of the bones occurred in disarticulation, and some were preserved as fragments. This kind of preservation suggests that the bones remained in subaerial conditions for a long time after death, before eventual burial occurred (Sereno *et al*, 2013). The bones were randomly deposited with no orientation or sorting. Post-mortem crystallization and mineralization have taken place in some bones, giving the fossils a whitish appearance when cleaned of the purplish hosting matrix. The mineralization formed a very hard crust around the bones, which causes difficulties in the removal of matrix. The removal of the matrix frequently resulted in damage to the surface of the bone. At the Wedding Hill bonebed, the preservation of the bones is mostly whitish mineralisation, which differs from preservation of bones at the Pimwe Hill and some other sites around the farm which is usually brown reddish. The presence of carbonate nodules and concretions suggests that the bones were preserved in a sediment that was saturated with carbonate minerals unlike in other sites where fossilization occurred in environments affected by iron minerals.

Figure 4.2. Diagram showing the foot bones of a sauropodomorph comprising the tibia, fibula, phalanges and an ungual in a purplish matrix. **Abbreviations: fbl**- fibula, **mtl**- metatarsal, **phl**- phalanges, **phx**- phalanx, **tib**- tibia, **ung**- ungual.

Articulated robust sauropodomorph limb bones.

The limb bones comprise of a tibia, fibula, metatarsals, a phalanx and an ungual, in articulation. Weathering had fragmented the bones though they still maintain their positions. The huge size of the foot bones suggest that they belong to a robust sauropodomorph dinosaur. Huge Late-Triassic dicynodonts like *Lisowicia* could be comparable in size but the bones don't have the resemblance.

Tibia

The tibia is a long bone, though the preparation to clear the matrix is still incomplete, its general outlook can be seen. It is approximately 550 mm in length and the mid shaft diameter is 240 mm. The bone is wider and more robust posteriorly than it is medially and anteriorly. It is thinner medially than it is on both ends. It is separated from the fibula along the diaphysis by a convex elongate gape.

Fibula

The fibula is approximately 540 mm long with a medial diameter of approximately 155 mm. This bone is slender compared to the tibia and is expanded on the articulating ends both anteriorly and distally giving it slightly subconvex outlines.

Metatarsals

Some sections of the bones are missing but basing on the available portions, estimates were made. Metatarsal 1 is approximately 220 mm, Metatarsal 2 is approximately 240 mm, number 3 is approximately 220 mm, and the metatarsal number 4 is approximately 150 mm.

Ungual

The ungual is slightly curved both on the dorsal and ventral views, giving it a subconvex appearance. It has an approximate length of 114 mm and a basal width of 75 mm.

Other disarticulated material from the Wedding Hill bonebed

Figure 4.3. Postcranial bones collected from a bonebed at the Wedding Hill in the Tuli Basin. Some limb bones from different individuals are displayed on the images shown above. (A) is a sauropodomorph humerus, (B) is a left ischium of a dinosaur. (C) sauropodomorph femur, (D1) calcaneus, (D2) centrum, (E) an indet bone

fragment, (F) femoral head of a small dinosaur. **Abbreviations**: **af**- articulatory surface for fibular; **ant**- anterior trochanter: **ast**- astragalus; **at**- articulatory surface for the tibia; **calc**- calcaneus; **cent**- centrum; **dpc**- deltopectoral crest; **fsh**- femoral shaft; **gtr**- greater trochanter; **hd**- femoral head; **ish**- ischium shaft; **raf**- radial fossa: **sul**- sulcus; **op**- obturator process.

Humerus

A sauropodomorph humerus is shown on figure 4.3.(A). The humerus is broken into two parts, on the shaft. The bone shows a distinct deltopectoral crest though its partly broken, it resembles sauropodomorph humerus. There is absence of distal expansion, but the bone is expanded, and sub flattened anteriorly from above medial region. Most sections of the humerus head are missing but its overall appearance suggests that it belonged to a medium-sized individual. The radial fossa is not prominent, it suggests it was a shallow depression on the distal end of the medial view, the radial condyle is present but not well pronounced. The length of the humerus measures 260 mm though some portions are missing while the shaft circumference is 150 mm. The distal end of the humerus is broken laterally along the distance between the radial fossa and the ulna condyle, and the latter portion is missing. The size of this humerus suggests strongly that it belongs to the articulated hindlimb of the large sauropodomorph collected in association with from the bonebed.

Left ischium.

The bonebed produced various post-cranial elements that included an ischium of a big individual Figure 4.3.(B). The ischium is long, cylindrical and has proximal axial sulcus, and shows moderate expansion. These characters are unlike those of the contemporary dicynodonts. The size of this bone suggests that it belongs to the larger taxon, probably a sauropodomorph. it measures 370 mm in length though some portions of anterior and distal pieces are missing. The shaft measures 190 mm to the start of the anterior curve and the curved portion is 180 mm in diameter.

Femur

A section of a femoral head of a sauropodomorph dinosaur was collected from the Wedding Hill and is displayed in Figure 4.3. (C). This femur is of large size and bears a distinct, finger-like lesser trochanter, this feature is a unique character for early branching sauropodomorph taxa The size of this femoral head suggests that it belonged to a big individual. The distance from the top of the humeral head to where the lesser trochanter starts is 110 mm. Due to erosion on some portions of the femur, only a partial length of the lessor trochanter remains while 4th trochanter portion broke off. The length of the femoral head is 160 mm.

Astragalus

The astragalus, shown in Figure 4.3 (D) 1, has a length measurement of 65 mm and measures 30 mm across its medial section. The astragalus is in articulation with the calcaneum.

Indet centrum

An indet small centrum is shown on Figure 4.3 (D) 2. The upper section that includes the neural spine and the transverse process is missing.

Femoral shaft

This bone is a fragment of a femur shaft just below the femoral head. The femora portion was affected by weathering, which destroyed parts of the bone, making it difficult to precisely identify it. The femoral portion occurred in association with various theropod bones which could suggest that it also could belong to a theropod. Figure 4.3., (E) shows the femur fragment. The damage caused by weathering on this bone meant no useful measurements could be obtained from it.

Small proximal femur

A femoral head of a small sauropodomorph is displayed on Figure 4.3, (F). This partial femur bears a combination of characters which are only present in sauropodomorphs, such as a tapering acute lateral edge to the greater trochanter, a transverse sulcus across the head, and a small finger-like anterior trochanter. The proximal section of the bone, that includes the femur head is preserved while the distal portion had been weathered away. The remaining portion of the proximal femur is 78 mm. Medial view of the femoral head presents a slightly curved surface.

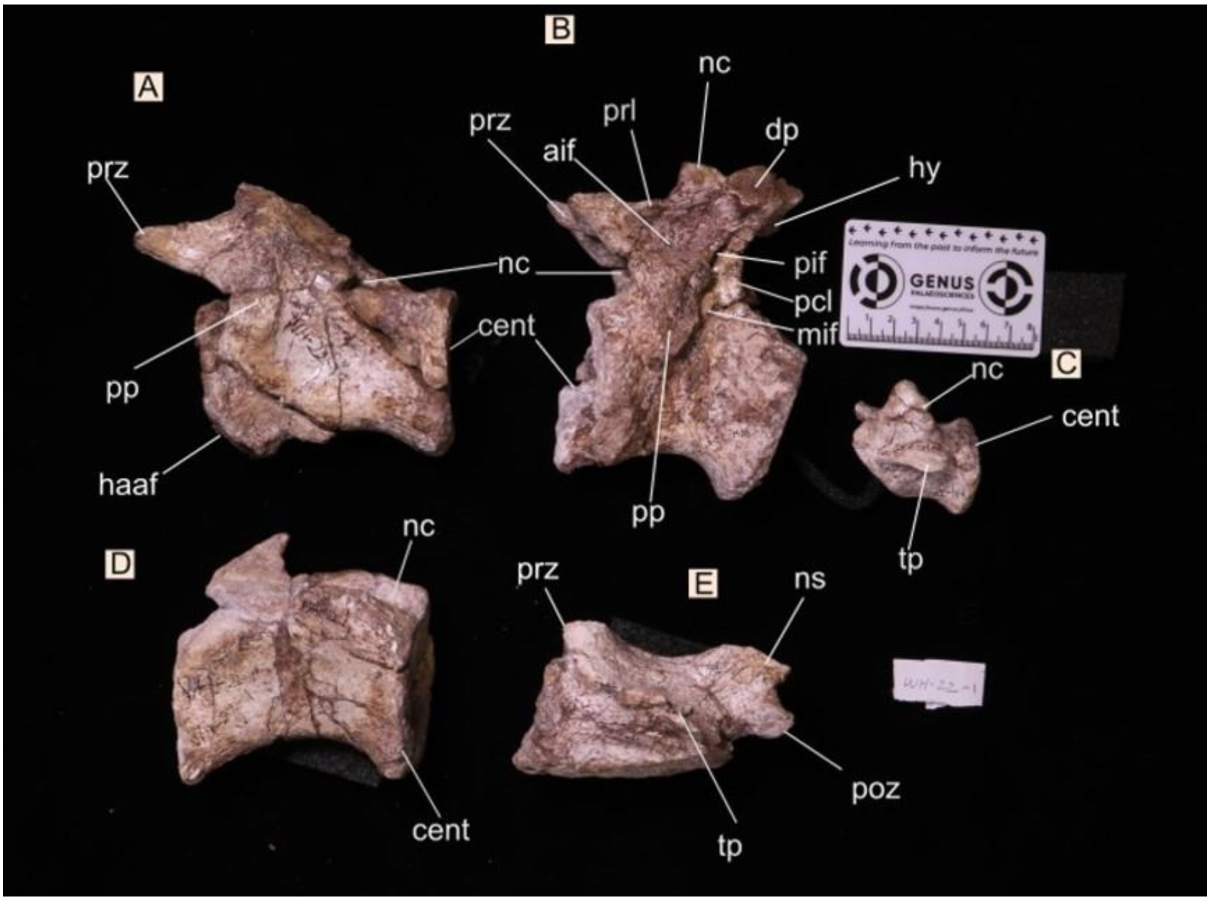

Figure 4.4. Sauropodomorph vertebrae and some vertebrae fragments, from a bonebed at the Wedding Hill. Figure (A) is caudal vertebra, (B) is a dorsal vertebra, (C) shows a section of the caudal vertebra. (D) is dorsal vertebra, while (E) displays a top section of a caudal vertebra**. Abbreviations**: **aif**- anterior infradiapophyseal fossa; **cen**- centrum; **dp**; diapophysis; haaf- haemal arch articular facet; **hy**-hyposphene; **mif**- middle infradiapophyseal fossa; **nc**- neural canal; **ns**- neural spine; **pcl**- posterior centrodiapophyseal lamina; **pif**- posterior infradiapophyseal fossa; **poz**- post zygapophysis; **pp**- parapophysis; prl- prezygodiapophyseal lamina; prz- prezygapophysis; **tp**-transverse process.

Caudal vertebra

The bone is weathered and is missing the upper parts and the posterior sections that include the remnant of the neural spine, and the postzygapophysis, the centrum is present. This vertebra is shown on Figure 4.4(A). On the articulatory facet of the anterior centrum, a haemal arch articular facet is present. The vertebra is amphicoelous, with the other articulatory facet deeply curved. Only a base of the transverse process remains. The length of the vertebra is 80 mm, height of anterior articulating surface is 70 mm, and the length of the neural arch is 65 mm.

Dorsal vertebra

Image (B) in Figure 4.4. shows a dorsal vertebra of a medium sized sauropodomorph. The vertebra is amphicoelous and the curve on the ventral edge gives a hook outlook, and the dorsal view is dome shaped with the upper elements of the vertebra stemming out on the central dorsal surface. Zygapophyseal lamina on the lateral side, the vertebra bears the diapophysis and the parapophysis as scars for rib attachment. In between the prezygapophysis and the transverse process, is an anterior infradiapophyseal fossa that appears prominently. There is also prezygodiapophyseal lamina providing an upper boundary for the fossa. In between the hyposphene and the transverse process there is the posterior infradiapophyseal fossa and medially, close to the diapophysis there is the middle infradiapophyseal fossa. Infradiapophyseal fossae in all archosaurs were functioning as pneumatic apparatus (Yates *et al*, 2012).

Caudal vertebra

A piece of caudal vertebra is shown in Figure 4.4(C), the bone is a fragment that preserves the basal portion of the neural spine and transverse processes. The proximal articulating surface of the centrum is eroded. The centrum is sub-rounded on the articulating surfaces and the neural canal filled with matrix.

Dorsal vertebra

A centrum of a dorsal vertebra is preserved and is shown on Figure 4.4 (D), this bone shows the base of the traverse process. This centrum is amphicoelous, with a length of the centrum is 95 mm, and the width of the undamaged centrum is 60 mm while the height of that end is 78 mm. Not much information can be obtained because of the incompleteness of the vertebra.

Caudal vertebra

The upper part of the caudal vertebra is shown on Figure 4.4. (E). A dorso-ventral compression occurred on the bone in addition to the damage on the ventral side. The neural canal is compressed and crushed dorso-ventrally. Basal remains of prezygapophysis, neural spine, traverse process, and basal potion of postzygapophysis is present on the vertebra fragment.

These vertebrae possess some features such as elongate centra, tall neural arch, several laminae and pronounced hyposphene / hypantrum articulation as in the case of the vertebra shown in image B, and with shallow amphicoelous, centra. In the late Triassic there are not many taxa of this size. The vertebrae are most probably sauropodomorph because of differences with other contemporary taxa of similar size like the huge dicynodonts and the large pseudosuchians. Caudal vertebrae of the former are much shorter anteroposteriorly and their dorsals don't bear laminae while the latter taxa bear vertebrae that are deeply spooled and highly concaved lateral surfaces. The basal theropods of the late-Triassic were not as large, in any case a theropod of this size would have deep pleurocoels on dorsal vertebrae and longer prezygapophysis.

Figure 4.5. Sauropodomorph indet vertebrae collected from the Wedding Hill site, most of the bones are weathered. (A), is a dorsal vertebra, (B) shows a segment of a centrum. Image C shows a caudal vertebra. Image (D) shows a caudal vertebra from mid sections of the tail while images (E) and (F) show posterior caudal vertebrae. **Abbreviations: cen**- centrum**; haaf**- haemal arch articular facet**; h**y- hyposphene; **ld**- lateral depression; **nc**- neural canal; **ns**- neural spine; **poz**- postzygapophysis; **prz**- prezygapophysis; **tp**-transverse process.

Dorsal and caudal vertebrae

The dorsal vertebra displayed in Figure 4.5. (A) bears deep curved articulating facets (amphicoelous) and an elongated centrum. The ventral edge of the vertebra is smoothly curved. Base of the neural spine is present and the postzygapophysis is preserved and bears a high neural arch. A caudal vertebra centrum with a lateral depression is shown in Figure 4.5.(C). The vertebra has the haemal arch articular facet, a hyposphene and the neural canal are preserved on this bone. This bone is laterally compressed, which gives the ventral view a narrow curve appearance. Image (B) is a fragment of a centrum and a small portion of transverse process. Image (D) is eroded but a small portion of transverse process is preserved. Images (E and F) are caudal vertebrae towards the distal end of the tail. They preserve bases of neural spines, elongated centra, traverse processes, pre and postzygapophysis, and neural canals are also present. Many of these vertebrae are weathered but they largely can be classified as indeterminate sauropodomorph.

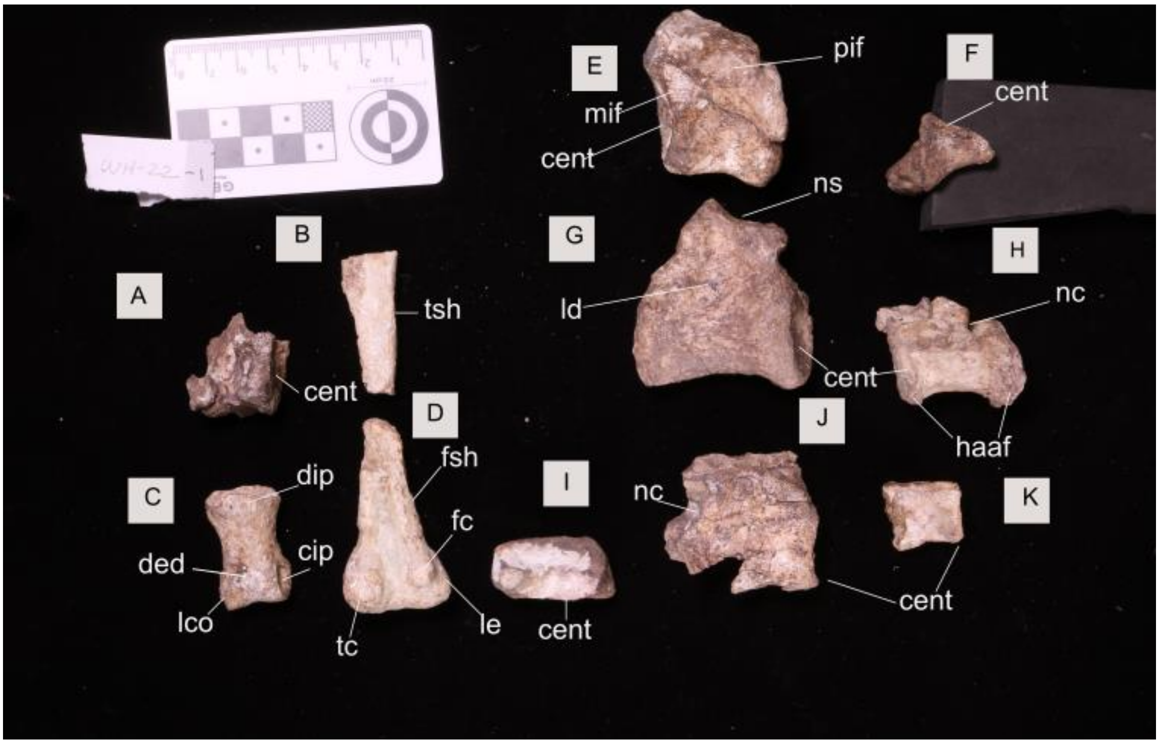

Figure 4.6. Postcranial bones from the Wedding Hill bone bed. (A) is a fragment of a vertebra of a small dinosaur, (B) The image displays a photograph of a fragment of a tibial shaft. (C) A phalanx is displayed while (D) shows a distal femoral end of a small dinosaur. (E) shows a dorsal vertebra. (F) shows a centrum of a small vertebra and (G) is a caudal vertebra, (H) also displays a caudal vertebra while (I, J, and K are also fragments of vertebrae). **Abbreviations**: **aif-** anterior infradiapophyseal fossa; **cen-** centrum; **clp-** lateral collateral ligament pit ;**ded-** dorsal extensor depression;

dip- dorsal intercondylar process; diapophysis; **fc**- fibular condyle; **fsh**- femoral shaft; **haaf**- haemal arch articular facet; **hy**- hyposphene; **ld**- lateral depression; **lco**- literal condyle; le- lateral expansion; **mif**- middle infradiapophyseal fossa; **nc**- neural canal; **ns**- neural spine; **pcl**- posterior centrodiapophyseal lamina; **pif**- posterior infradiapophyseal fossa; **poz**- post zygapophysis; **pp**- parapophysis; **prl**- prezygodiapophyseal lamina; **prz**- prezygapophysis; **tc**- tibial condyle; **tp**-transverse process; tsh- tibia shaft.

Image (A) can only be identified as dinosaurian indet partial vertebra.

Tibia shaft

A small tibia shaft is shown on image (B). This partial shaft is strongly flattened, and it suggests that it could be a theropod or an ornithischian but not a sauropodomorph because of this strong flattening.

Pedal phalanx

Image (C) displays a pedal phalanx; this bone cannot be identified to a lower taxonomic level.

Distal femur

This distal femur shown in image (D) has a tibiofibular crest present and because of this feature, the distal femur is likely of a small dinosaur or a late branching pseudosuchian. The shape of this bone resembles those of dinosaurs, it lacks the deep patella depression on the surface and possible bears a small mediodistal crest- a character only present in theropods. Erosion has damaged the surface of the bone though the described features can still be seen. The width of this distal end across condyles is 30 mm, with a thickness of 20 mm. The gape in between the tibial and the fibula condyles is slightly wider than the width of the fibula condyle. The medial view of the distal femur on the tibia condyle lateral end, shows a sub-rounded outlook while on the side of the lateral expansion, it gives a slightly straightened view. In relation to the fibular condyle, the tibial condyle is wider, with sub straightened surface and slightly inclined towards the medial gap. The fibular condyle is narrow doom-shaped, while the overall dorsal view of the whole distal femur shows a little sub-curved appearance.

Vertebrae

Images (I - J) in Figure 4.6 These partial vertebrae were affected by weathering and fragmentation which rendered them difficult to describe but, basing on their size, they are most likely dinosaurian, they don't possess distinguishing characters for contemporary taxa such as either dicynodonts or pseudosuchians as mentioned earlier. They lack sufficient features

Vertebra centrum shown in image (K) is dinosaurian indet of a small individual but lacks distinguishing characters for further classification. The centrum is elongated and amphicoelous.

Image G shows a vertebra with a rounded centrum and articulating surface. The base of the neural spine is preserved. On the medial portion there is a gorge on the lateral surface below the transverse process. This gorge is the lateral depression. The transverse process is not preserved. Image (F) is a broken vertebra, showing only the articulating end of the centrum. (H) is a caudal vertebra that has haemal arch articulating facet on both ends while image (K) shows a dorsal vertebra centrum that misses the part of the centrum.

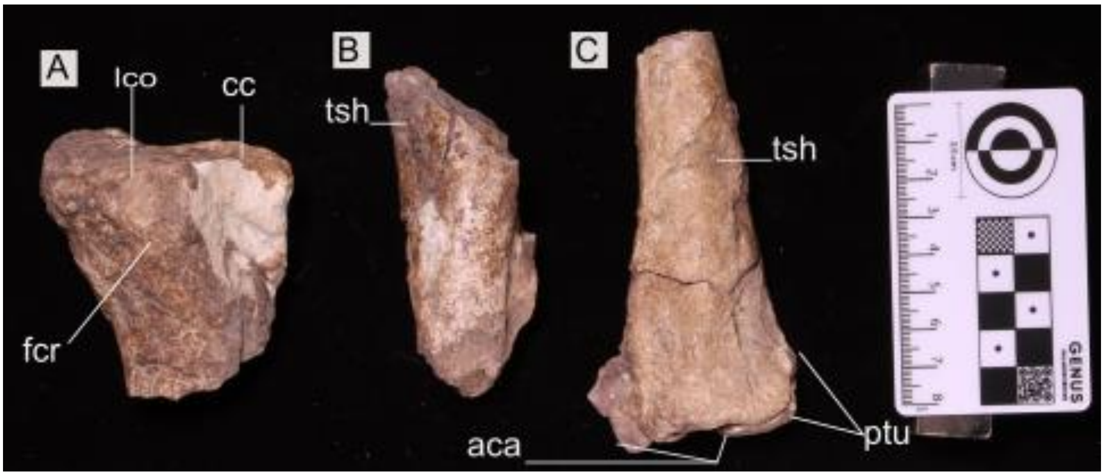

Figure 4.7. Fragments of tibia of a medium-sized theropod dinosaur collected from the bonebed at the Wedding Hill. A proximal end of a tibia is displayed in (A), image (B) shows a tibial shaft, and the distal end is displayed in image(C). **Abbreviations**:

aca- articular surface for the calcaneum; **cc**- cnemial crest; **fcr**- fibular crest; **lco**- lateral condyle; **ptu**- posterior tuberosity; **tsh**- tibial shaft.

Tibia

Fragments of a Theropod tibia were collected from the bonebed at the Wedding hill and Figure 4.7.(A) displays the proximal part. This bone is smoothly curved posterolateral and has a well-developed cnemial crest that extends prominently posteriorly, identifying it as a dinosaur. The front side of a dorsal view is raised higher than the back. There is also a distally extending fibula crest and a lateral condyle, which is a defining character in early branching theropods. Image (B) is a tibial shaft, probably belonging together with the proximal fragment and the distal tibia shown on image (C). The distal tibia is flattened anteroposteriorly and has a facet for articulation of the ascending process of the astragalus, it bears a posterior tuberosity which is box-like for the attachment of the calcaneum and fibula. These characters are also exclusive to theropods. All these bones came from the same quarry, and they appear proportional to each other. It would be reasonable to deduce that they belong to the same part of the limb, based on quarry position, preservation and size. These tibia fragments were broken by weathering processes.

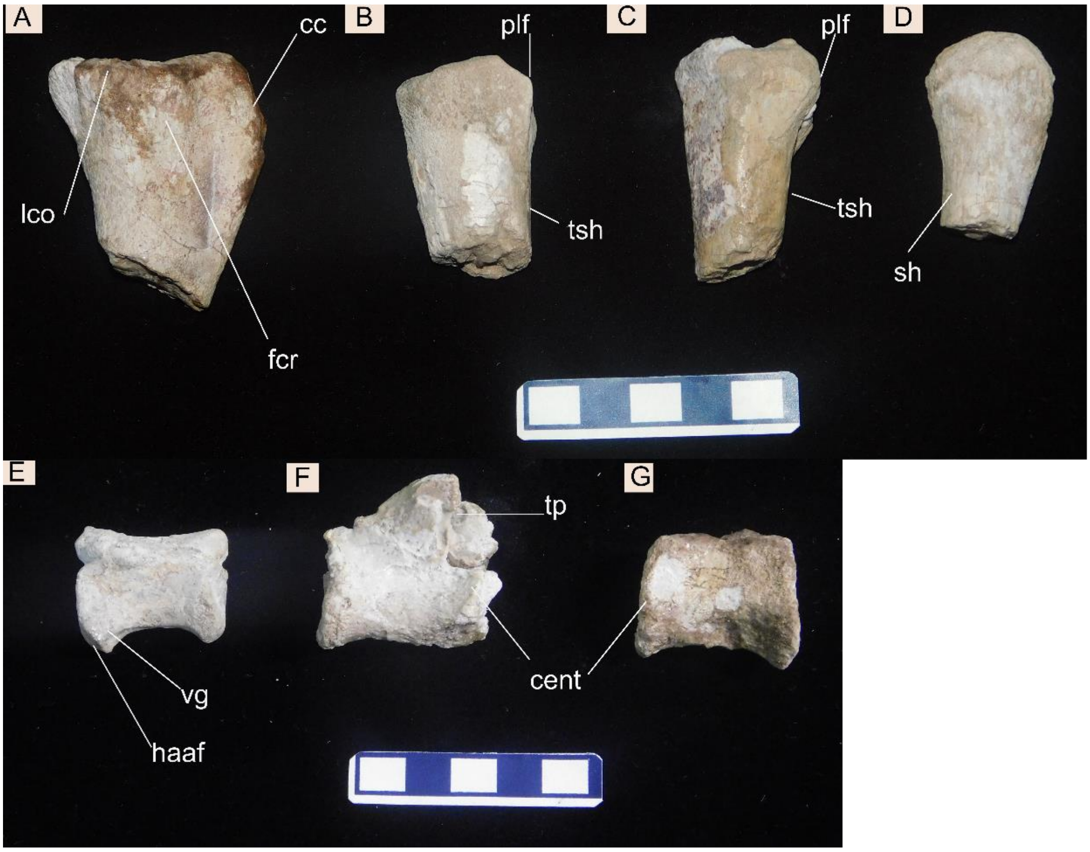

Figure 4.8. Bones of a small dinosaur from the Wedding Hill bonebed (A) a theropod proximal tibia, (B and C) theropod distal tibia, an indet bone (D), (E – G) these are caudal vertebrae of indeterminate reptile. **Abbreviations**: **aca**- articular surface for the calcaneum; **cc**- cnemial crest; **cent**- centrum; **fcr**- fibular crest; **haaf**- haemal arch articulating facet; **lco**- lateral condyle; **mm**- mesial margin; **plf**- posterolateral flange; **sh**- shaft; **tp** - transverse process; **tsh**- tibial shaft; **vg**- ventral groove.

Proximal tibia

A small theropod tibia fragment is shown on Figure 4.8 (A), the tibia portion is a small bone that is slightly curved posteroventral. It has a prominent cnemial crest that is smoothly curved, giving an overall curved morphology to the tibial portion. The fibula crest is preserved on a much more robust section medially at the anterior end of the bone. The lateral condyle is also preserved ventrally to the fibula crest, conditions characteristic of theropod dinosaurs, The cross-sectional view of the shaft has a sub-oval shape.

Distal tibia

In diagrams (B and C) in Figure 4.8. are distal tibial ends of small dinosaurs, probable of theropods. The bones were preserved in hard mineralised matrix. The bones are hollow but filled with calcite minerals. Both bones are left distal tibia, suggesting that there was more than one individual circumference of tibia (B) is 68 mm and that of bone (C) is 57 mm. The diameter of the hollow part of B is 13 mm while that of (C) is 10 mm. All the two bones exhibit similar morphology. They are broader on the posterior and flat laterally, suggesting they are theropods.

Indeterminate bone

The bone displayed on Figure 4.8.(D) is sub curved and with a sub rounded circumference. It is also hollow and filled with calcite minerals. Across the hollow section, the bone is mm in diameter, while the circumference measures mm. The bone shows a smoothly rounded but eroded end. The bone was collected in association with the small animal bones from the Wedding Hill.

Caudal vertebra

On this centrum shown on Figure 4.8.(E), only the centrum of a caudal is preserved, the base for the attachment of the prezygapophysis, postzygapophysis, traverse process and the neural arch can be seen on the dorsal surface of the bone. This bone has haemal articulating facets on both ends and ventral groove is also present, stretching the whole length of the ventral side of the centrum. The length of the vertebra is 30 mm, the height of the centrum at one end is 20 mm, width is 17 mm, and the other is side is 16 mm and width are 17mm respectively.

Caudal vertebrae

In Figure 4.8.(images F and G) are caudal vertebrae of a small reptile also from the Wedding Hill bone bed. In (F), the vertebra has one side of a transverse process but is also not complete. The transverse process is damaged by mineralisation, the distal articulating facet of the centrum is partly broken. The vertebrae seem not to have articulating facets for ribs and chevrons.

Image (G) shows a centrum which lacks the other parts that had been weathered away. On both bones, the surface bone had been affected by mineralization and weathering.

Postcranial bones collected by the Bristow family from the Pimwe Hill

Several postcranial bones were collected by the Bristow family from the Pimwe Hill and are kept at their fossil display room. The bones comprise of an almost complete vertebrae column and some elements of limb bones. There are 3 femora of different sizes suggesting that there were probably 2 or 3 individuals at the site since the bones were found together. The bones were discovered after a heavy rain caused massive erosion on the outcrops at Sentinel Ranch. Most bones seem to be covered in haematitic matrix. This suggest preservation in subaerial and hot environment, the bones are displayed in Figure 4.9. The sizes of the limb bones from this collection are smaller than the limb bones of a robust sauropodomorph collected from the Wedding Hill bonebed. The size of these bones suggests that they could belong to a medium sized sauropodomorph. Some of the vertebrae are still articulated and seem they had fused epiphysis, which suggests that they were adults. There are a few bones broken on the epiphysis suggesting that they were sub adults.

Figure 4.9. Sauropodomorph postcranial bones collected from the Pimwe Hill. Images (A – A4) are indeterminate bone fragments, (A5 – A6) are rib fragments, (B - B5) are also indeterminate bones. (C) is an astragalus of an indet dinosaur, (D) is an indet bone, (E) is an indet sauropodomorph distal femur in posterior view, images (F and G) are sauropodomorph pubes, (H) is a sauropodomorph caudal vertebra, Images (I – I2) are indet bone fragments, (J – J4) is a distal femur and associated shaft fragments, (K – K4) are indet bone fragments, (L – L4) are indet bones, (M – M6) are sauropodomorph dorsal vertebra, (N) is an astragalus of a medium-sized reptile, (N1 – N4) are indet reptile bones , (O – O3) indet bones, (P and P2) are unguals of indet reptile bones, (P1, P3 – P6) are phalanges of indet sauropodomorph, (Q) indet sauropodomorph femur in dorsal view, (R – R16) caudal vertebrae of indet sauropodomorph.

Astragalus

Image (C) displays a robust astragalus which is likely sauropodomorph because of its size and its association with the other material which is probably sauropodomorph.

Femora

Images (E, J, Q) display some femora. a distal femur is displayed in image (E). Both the fibula and tibia condyles on this partial femur are pronounced, the partial shaft looks flattened, broad and a bit gracile in relation to the pronounced condyles. In image (J) a distal femoral portion is displayed together with associated femoral shaft sub cylindrical fragments (J1 -J4). A femur is partially shown in image (Q). This femur looks sauropodan sadly many details are cut-off on the image. The femur is robust and most likely of a dinosaur because of its size and its association with other bones identified as sauropodomorph from the same location.

Pubes

Pubes are shown in images (F and G), these bones are of the same size and bear some unique features that suggest they are sauropodomorph dinosaurs. The pubes are mediolaterally expanded and proximodistally straight, with a small distal expansion. These characters are exclusive to sauropodomorph dinosaurs.

Vertebrae

(M and R numbers) The vertebrae seem to be generally slightly flattened on the centra, the dorsal vertebrae appear to be laterally elongate while the length of the centra and their heights are almost similar in the caudal vertebrae. They become laterally compressed from (R6) and the posterior ones. Some vertebrae are articulated and appear as blocks with 2 or 3 articulated bones. The caudal vertebrae (with R numbers) bear haemal arc articulating surfaces for the articulation of chevrons (the bones arranged under these caudal vertebrae). The vertebrae also lack deep spooling on the centra. This suggests that these vertebrae can't be assigned to pseudosuchian material and because of the length of the tail on Figure 4.9, which is quite long, suggests that these can't even belong to large dicynodonts which bear much shorter tails. The vertebrae are most likely of a medium-sized sauropodomorph.

CHAPTER 5

Dating of Beds

Sentinel Ranch zircon samples

The results from the LA-ICPMS analysis are displayed in diagrams shown on Figure 5.1. Diagrams A and A1 show Concordia and kernel density estimations (KDE) curves respectively, derived from analysis of a sample collected from the Wedding Hill. The youngest U-Pb dates from zircons were used to infer the maximum depositional age (MDA) of the exposed Mpandi Formation beds at Sentinel. A sedimentary unit cannot be older than its youngest detrital zircon (Howard, 2023). The results from a Wedding Hill sample gave the youngest age of 202.7 ± 2.9 Ma. The distribution and the age range of the zircon crystals are displayed on the KDE graph with a range from 202.7 ± 2.9 Ma to 3250 Ma.

Concordia and KDE curves from a Pimwe Hill sample are represented by diagrams B and B1 respectively. The sample was collected from the basal sections of the outcrop, dominated by fine-grained massive sandstones which show feint horizontal bedding on upper sections of the bed. The MDA from this sample is represented by the youngest zircon crystal at 207.6 ± 4.6 Ma., this information is shown on the KDE graph which shows some peaks at 250 Ma, 500 Ma, 1000 Ma, 2000 Ma and at 3000 Ma.

The Rogers *et al* (2004) publication noted vertebrate fossils at the Old Homestead site, and we also sampled the site for age assessment using the U-Pb detrital zircon methods. The results for the old homestead Limpopo Riverbank sample are shown in diagram C and C1. This sample produced an MDA represented by the youngest zircon crystal of the Jurassic age at 199.2 ± 5.1 Ma. The detrital zircon ages range from 199.2 Ma to more than 3000 Ma. The KDE graph shows some peaks at around 250 Ma, 500 Ma, 1000 Ma, 1500 Ma, 2000 Ma and at 3000 Ma. This pattern is observed across the samples from the three localities where logging was done at the Sentinel Ranch. Major peaks are between 250 Ma ago and 1000 Ma.

At Barkley Pass in the Elliot Formation, U-Pb dating using detrital zircons gave an MDA of 208.80 ± 0.14 Ma, close to the base of the section and 194.65 ± 0.13 Ma near the top (Howard, 2023). These results are comparable to the MDA that were produced by the analyses of detrital zircons from the Mpandi Formation beds though the Mpandi Formation results could not produce younging-up zircons. The results suggest that the exposed Mpandi Formation sediments range in age from the late Triassic to the early Jurassic (Rogers *et al*, 2004).

The Late Triassic to Early Jurassic time interval records some crucial events in the earth history such as the eruption of the Central Atlantic Magnetic Province (CAMP-201.566 to 200.916 Ma), there was also the end-Triassic extinction (ETE) at 201.564 ± 0.015 Ma and the Triassic-Jurassic boundary at 201. 464 ± 0.004 Ma (Howard, 2023).

The 500 Ma peak corresponds to the age of kimberlite intrusion, 1000 Ma the Umkhondo LIP, 2000 Ma trans-Limpopo metamorphic event, - +2500-2700 Ma Bulai Granite and Limpopo deformation, and 3000 Ma older Limpopo gneisses, e.g. Sand River (Watkeys, 1979).

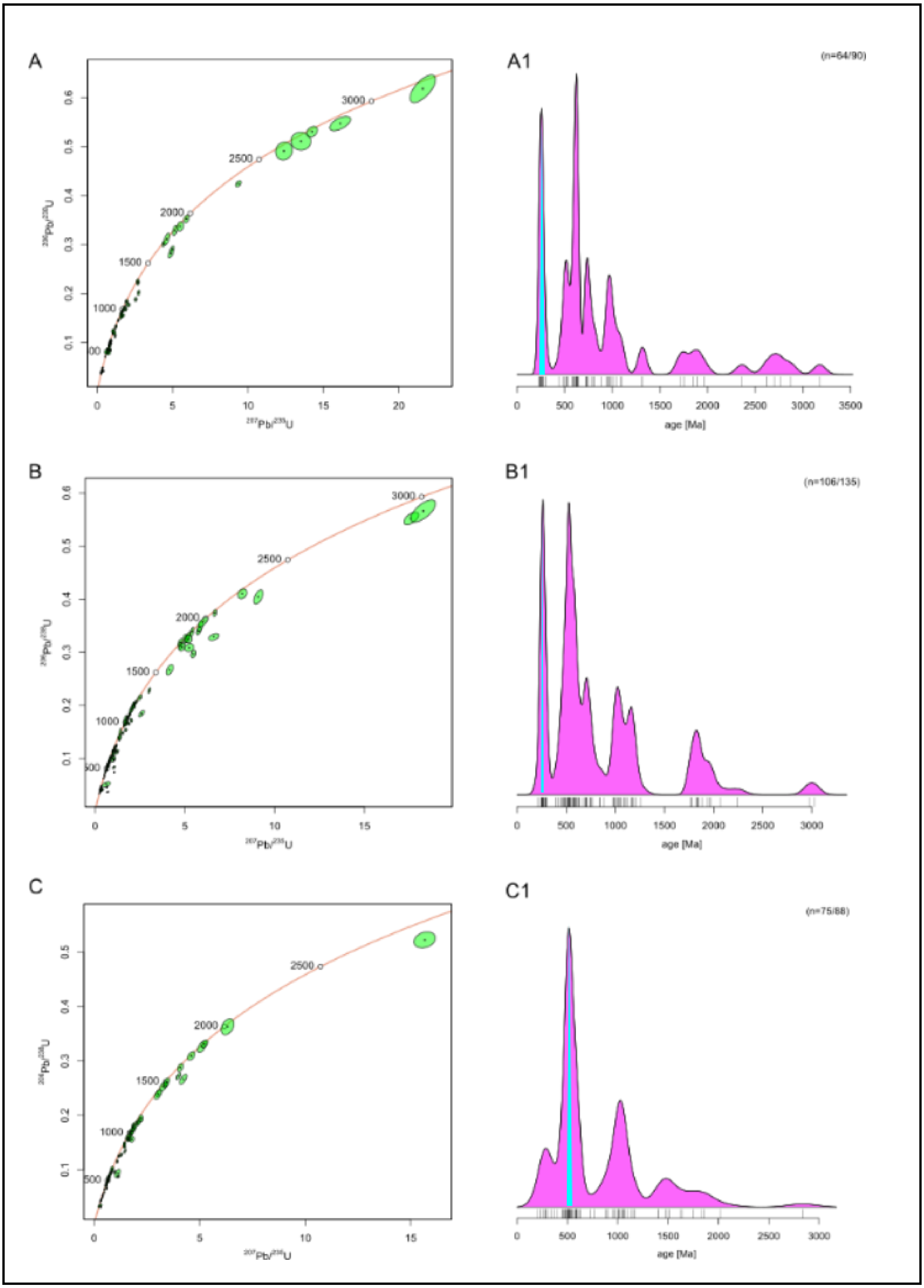
A
A1
(n=64/90)
B
B1
(n=106/135)
C
C1
(n=75/88)
$^{206}Pb/^{238}U$
$^{207}Pb/^{235}U$
age [Ma]
3000
2500
2000
1500
1000
500

Figure. 5.1. Diagrams showing Concordia curves and KDE graphs from LA-ICPMS analysis results of Wedding Hill, Pimwe Hill and old homestead Limpopo detrital zircon samples. Young zircons (< 232.5 Ma) are shaded in blue.

Table 5.1. Detrital zircon age-range and distribution from the LA-ICPMS analysis for the Sentinel samples.

No	**Site**	**Sample**	**Youngest zircon. Ma**	**Error ±**	**Number of Jurassic age occurrences**	**Number of Triassic age occurrences**	**Maximum age Ma**
1	Old Limpopo homestead	Limpopo - DZ	199.2	5.1	1	0	2710
2	Old Limpopo homestead	Limpopo -DZ1	220.1	8.7	0	2	2624
3	Old Limpopo homestead	Limpopo - DZ2	200.8	5.8	1	2	2610
4	Wedding Hill	WH-21D-1	202.7	2.9	0	10	1945
5	Wedding Hill	WH-21H-2	203.1	5.2	0	9	2696
6	Wedding Hill	WH-21H-3	204.1	3.9	0	3	1179
7	Wedding Hill	WH-21H-4	232.1	3.7	0	1	2562
8	Pimwe Hill	PW-22D-1-2	207.6	4.6	0	8	2891

CHAPTER 6

Boreholes

This chapter shows stratigraphically how the borehole sections relate to the total Mpandi Formation beds. Maximum thickness of the section is estimated, how much of that thickness is represented in outcrops, and where the fossils sit in relationship to that thickness.

In the study area, only upper sections of the Mpandi Formation beds, the Forest Sandstone Formation and the capping basalts are exposed whilst the lower beds including the lower Karoo equivalent rocks are buried under the ground. Unlike the sedimentary successions at the Main Karoo Basin where several hundreds of metres are exposed, the Tuli Basin successions were affected by numerous faults that effectively pushed the Karoo rocks down (Vail *et al*, 1969). To understand the stratigraphy and the sedimentology of the whole sequency, the use of borehole logs was therefore important and inevitable in this study. Historical borehole data adopted from Thompson (1975) were used, from 5 boreholes, which are all located on the east of the study area, within the boundaries of the Nottingham Estate Figure 6.1. Boreholes MRD1, T4, T5, T6, and T7 were used.

Despite all boreholes being located outside the Sentinel Ranch, they still provide important insight into the sedimentology of the buried strata as shown in logs on Figure 6.2. The Borehole MRD1 is located at UTM grid reference QF 686542 and with a collar elevation of 524 metres above mean sea level (msl) on the 2229B1 1:50 000-scale map of Zimbabwe, it is located NE of sentinel Ranch close to the boundary with Nottingham Ranch. This borehole is the deepest with a depth of 465.8 metres. It cuts through all the successions of the karoo formations (i.e. Forest Sandstone, Mpandi, Gushu, Fulton's Drift, and Dwyka beds). It also cuts through the overlying basaltic rocks, and gets into the basal gneiss rocks (Thompson, 1975). MRD1 is closer to the location of some of the fossil sites than all the other boreholes, with borehole T5 being the furthest.

Borehole T7 is roughly east of the Sentinel Ranch, and is on QF 700524, with a collar elevation of masl 496. This borehole is 119.7 metres deep. Borehole T7 was sunk on Fulton's drift mudstones, and it went down-to the basal gneiss rocks. Borehole T6, is the second deepest with a depth of 198. 73 metres. It is at QF 780568 with an elevation of 534 masl. This borehole was sunk through a section of the Mpandi Formation and transcends through the Gushu Formation to the Fulton's Drift Formation beds. The log ended on the gneiss rocks.

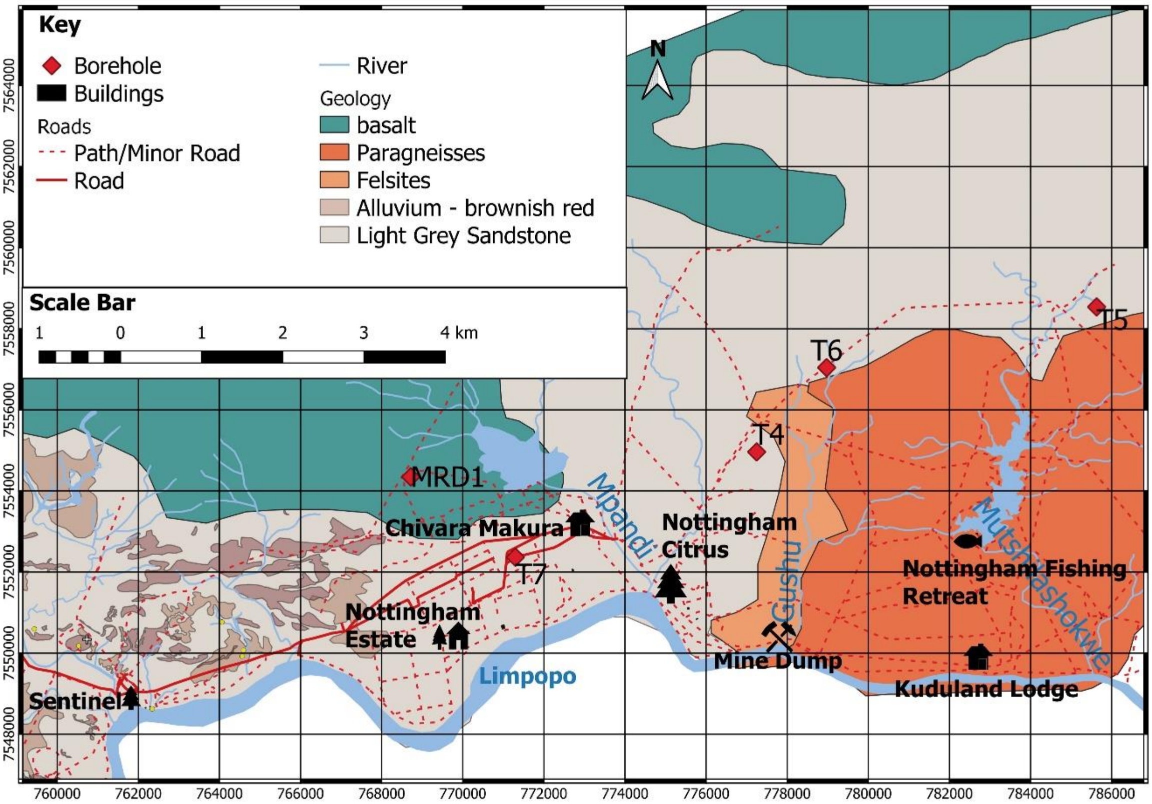

Figure 6.1. Map showing the locations of the 5 boreholes whose bore logs were analysed. They generally lie on an east to west direction, with all of them located in Nottingham Ranch.

Borehole T5 is also located on the east of the Sentinel Ranch and is the furthest, situated at QF 844584, elevated at 510 masl on 2229B2. The borehole is 114.91 metres deep and was drilled on the Mpandi sediments. Borehole T5 goes through a succession of the Karoo equivalent rocks from the Mpandi Formation to the Fulton's Drift Formation. The drilling of this borehole ended in an intrusive dolerite rock. Borehole T4 is located at QF 762547, 510 msl and is also east of the study area. It is located on map 2229B1.

Only borehole MRD1 shows the complete sequence of the stratigraphic units of the Karoo lithostratigraphic structure from the basal Dwyka beds to the capping basalts. It was sunk through the olivine basalts and the underlying Forest Sandstones where it showed that some thin sandstone layers were interbedded with some lava flows. The Forest Sandstone appears whitish on this borehole log. All the other boreholes were sunk on the lower formations and all of them including MRD1 went through to the basement rocks except for T4, which terminated in dolerite.

The upper sections of the boreholes are dominated by very fine-grained sandstones and marls, which may appear in various colours such as white, pink, green, purple, and these may appear in different shades of the colours. In the mid-sections of the borehole logs, the lithology becomes gritty and pebbly, intercalation of marl, conglomerates and mudstones may be present (Thompson, 1975). The basal portions are characterised by the dominance of shales which may be black, dark, and grey in colour. There are also thin sediments of coal occurring in alternating fashion with the shale sediments. Dolerite intrusions are also present in some borehole logs such as borehole T5 and the coal beds had not been encountered when the drilling ended.

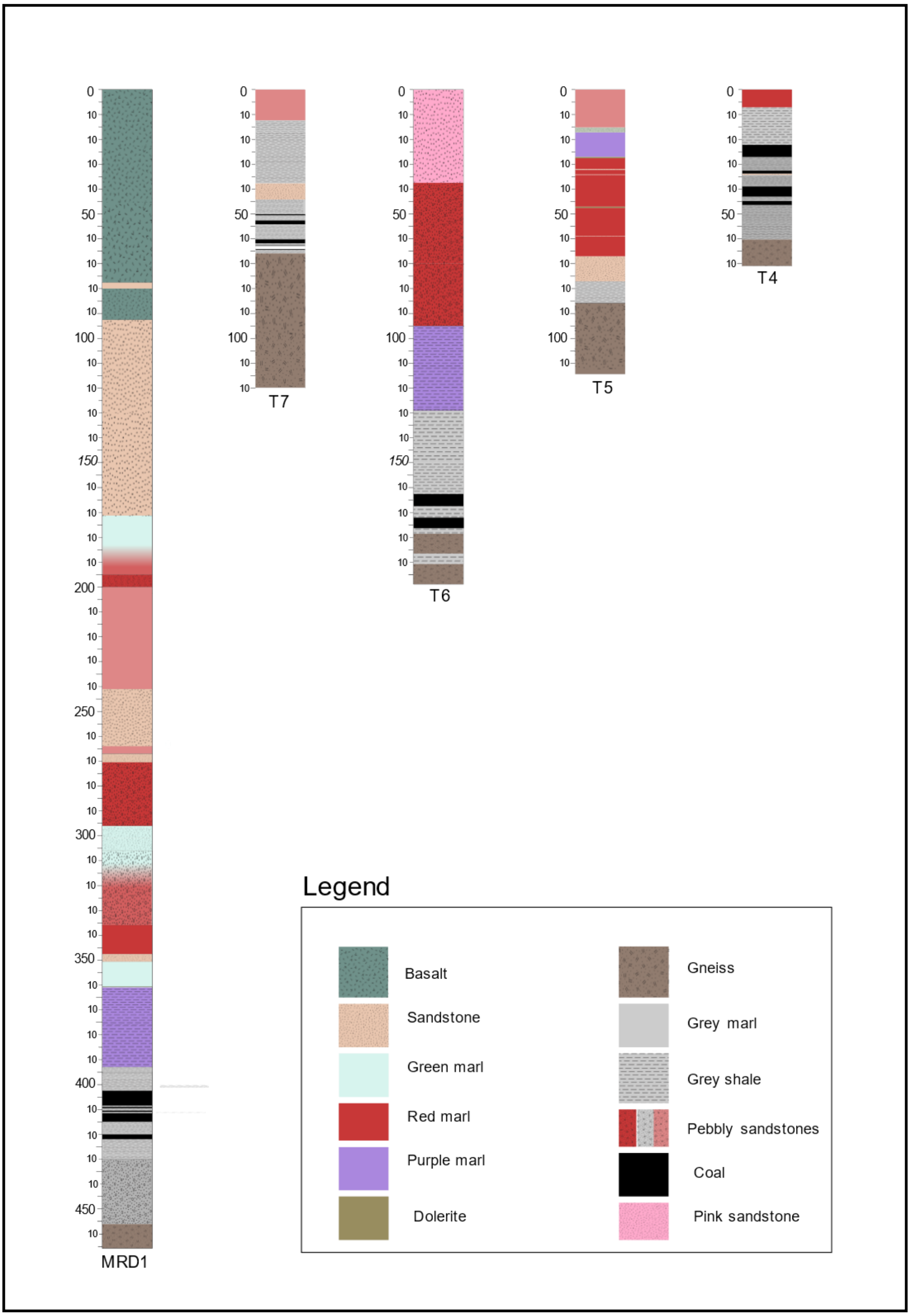

Figure 6.2. The re-drawn borehole logs modified after Thompson, 1975.

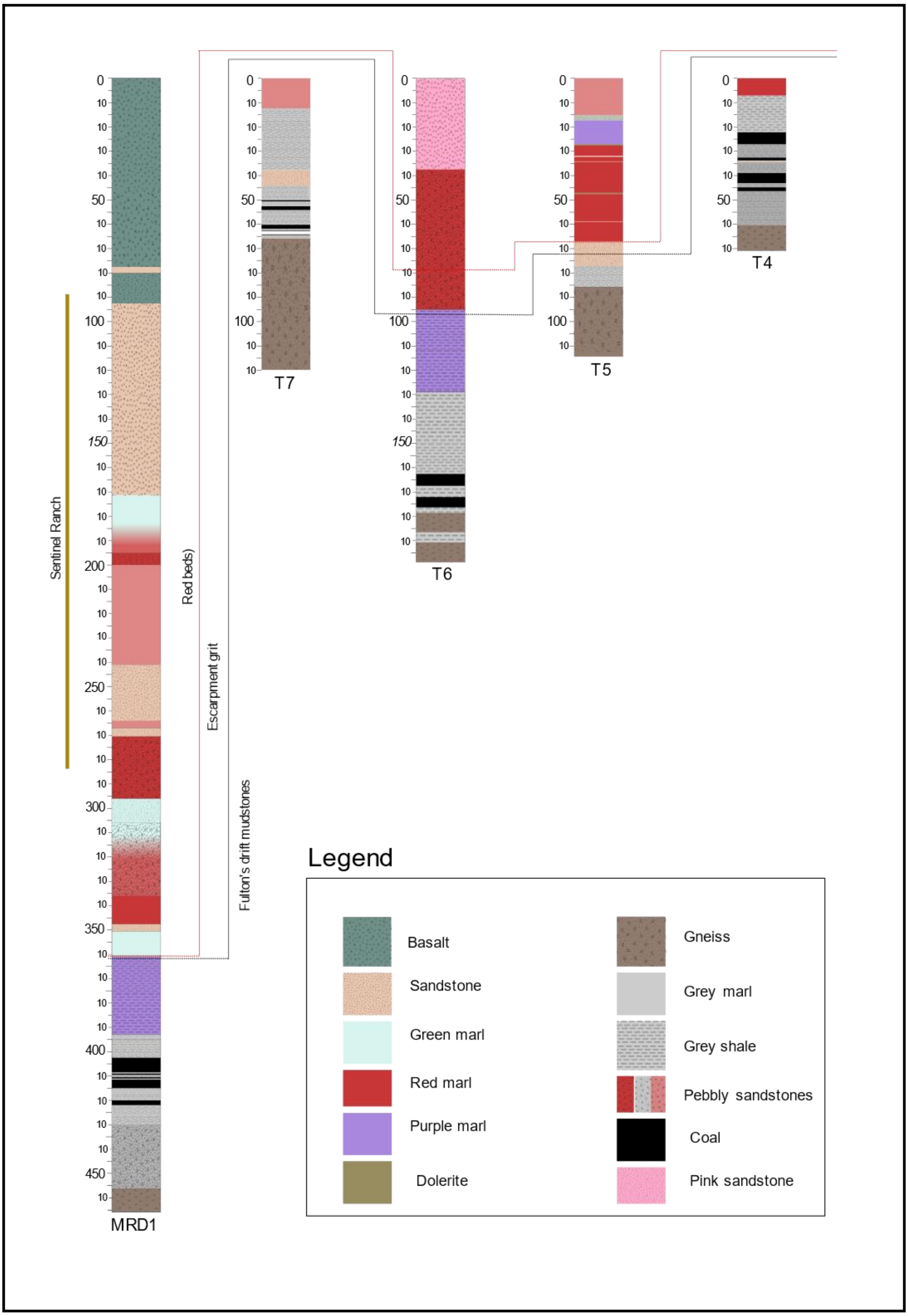

Figure 6.3. Borehole logs, showing estimated correlations to each other. Only borehole T5 did not encounter coal seams.

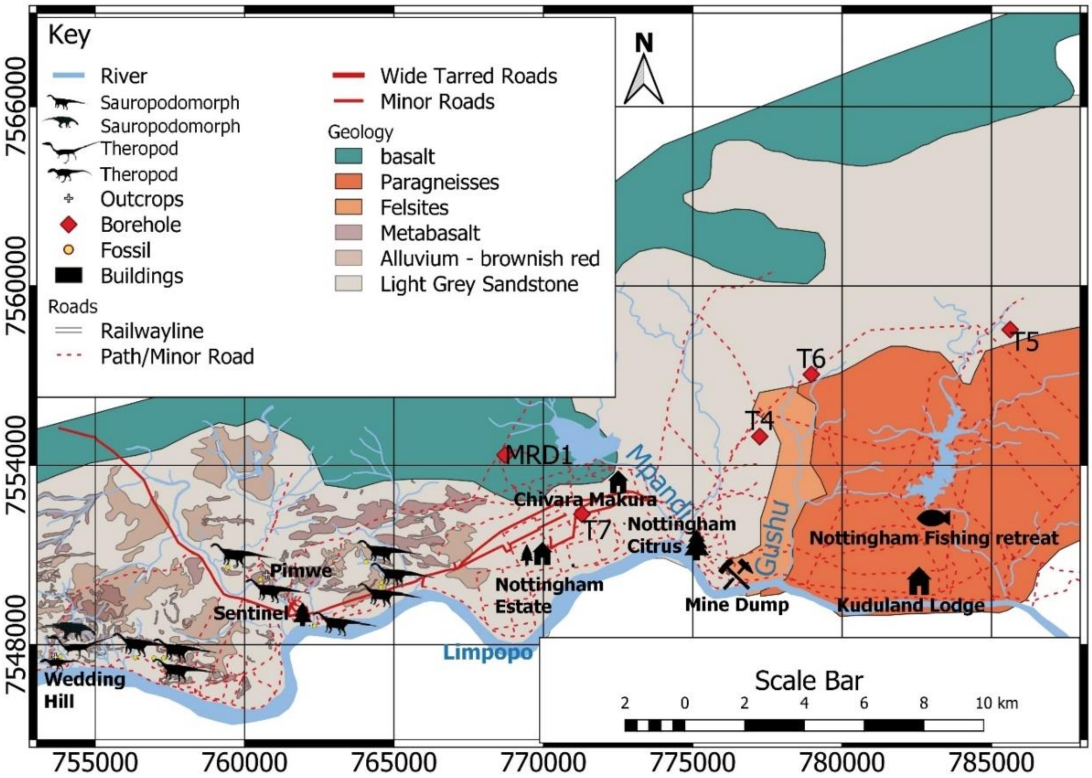

Figure 6.4. Location of boreholes in relation to the location of main fossil sites.

The maximum thickness of the Mpandi sediments as revealed by the borehole data.

The Mpandi formation thickness ranges from approximately 190 metres to approximately 65 metres, meaning that at least 100 metres is totally unexposed at Sentinel Ranch. Of this thickness, about 60 metres is represented by outcrops and is the thickness that is accessible for surface observations. Although the maximum thickness of the red beds is indicated as 360 metres, it includes the thickness of the Forest Sandstone and the overlying basalts at MRD1. The thickness of Mpandi Formation is the total thickness of the red beds less that of the Forest Sandstone and the basalts. The information suggests that surface field observations have only been done on the upper Mpandi Formation. Vertebrate fossils have been found at horizons below the 65 metres. This suggests that the Mpandi formation that can possibly be explored for fossils in the entire Tuli Basin is less than 65 metres and at the Sentinel Ranch is approximately up-to 54 metres because the 60-metre height of the Pimwe Hill also includes the Forest sandstone Formation beds and the capping basalts.

CHAPTER 7

Discussion

Stratigraphic sections and sedimentary structures

The stratigraphic sections show that the Mpandi Formation is dominated by very fine-grained sediments which tend to feature calcareous nodules, and occasionally infraformational conglomeratic sediments also occur as beds of up-to 60cm in thickness. The fine sediments are usually silty sandstones, siltstones or mudstones ranging in different shades of red/purple and at times pink colours (Thompson, 1975; Rogers *et al*, 2004). Medium-grained to very fine-grained sandstones are also present, usually in brownish or pinkish colours, commonly occupying basal portions of the outcrops. The colour of the fine sediments tends to become greyish in the upper beds where they culminate to silicification into silcrete towards the contact with the overlying Forest sandstone Formation (Robertson, 1967; Bordy, 2000). The fine-grained sediments in some cases bear mud clasts, mud drapes, desiccation cracks and silicified root traces as well as vertebrate fossils (Robertson, 1967).

At the Wedding Hill, vertebrate fossil bones were discovered at a fine-grained purplish bonebed underlying a transformational conglomerate, while at Pimwe Hill, fossils were recovered from two horizons, at a lower fine-grained red bed at ~ 8m and on a transformational conglomerate sediment lying higher on stratigraphic section at ~ 32m. The transformational conglomerate beds are clast supported, with fine-grained matrix, finning-up at Wedding Hill, and unsorted at Pimwe Hill. Bioturbation occasionally occurs in sandstones and fine beds at Pimwe Hill.

There are very close similarities in these sedimentology features of the Mpandi Formation in comparison with those of the Elliot Formation in the main Karoo Basin (Bordy, 2000; Bordy and Catuneanu, 2001; Bordy *et al*, 2004; Bordy and Eriksson, 2015). In the Elliot Formation, it was noted that the Lower Elliot Formation is massive, with cross stratified beds and is sandier in comparison to the tabular, sheet-laminated siltier, Upper Elliot Formation (Bordy *et al*, 2004). These are postulated to have been deposited through different depositional fluvial styles. The Lower Elliot Formation through perennial meandering fluvial systems and the Upper Elliot Formation through ephemeral fluvial styles (Bordy *et al*, 2004). The Mpandi Formation also shows a general finning-upward trend, and it can be inferred that the depositional processes were similar.

The fine-grained sediments, include siltstones, mudstones and very fine sandstones, are the most prevalent in the Mpandi Formation. The fines are common in overbank environments, and they constitute deposition from suspension as overbank and flood plain deposits. They may be deposited from lakes and ponds (Bordy, 2000; Rogers *et al*, 2004 Miall, 2006). Infraformational conglomerates were also observed in the Mpandi Formation. These are pseudo-plastic debris flows which were deposited by viscous, laminar or turbulent flows (Bordy, 2000; Miall, 2006).

The other common lithofacies in the Mpandi Formation are the massive fine to medium-grained sandstones. These are sediment gravity flow deposits usually characteristic of small channels. Some beds show feint bedding while others appear to be just massive. This would suggest that some Mpandi beds were deposited as sediment gravity flow deposits in small channels (Miall, 2006).

The horizontally bedded sandstones are also found in the Mpandi Formation though not very common. These may occur in shallow water where the velocity is low, and the sand is very fine to medium-grained sands (Miall, 2006). Trough cross-beds and planner cross-beds occur but they were very uncommon. The former forms through migration of dunes where the rate of sedimentation is very low (Bordy, 2000). The occurrence of these facies in the Mpandi Formation, closely corresponds to the occurrence of relatively similar facies in the Elliot Formation (Thompson, 1975; Bordy, 2004, Bordy, 2015).

Boreholes

From the boreholes data it could be deduced that the Mpandi Formation has a maximum thickness of approximately 190 metres. The approximate thickness of the outcrops is 65 metres for the Tuli Basin, and 60 metres for the thickness of outcrops at the Sentinel Ranch with Pimwe Hill being the highest. This is quite thin when compared to the thickness of outcrops and exposures available for fossil exploration at the Main Karoo Basin where hundreds of metres are exposed. This Suggests that at least 100 metres of the lower beds of the Mpandi Formation are totally unexposed within the environs of Sentinel Ranch.

These results reveal that there is a deep history of deposition in the Mpandi Formation that does not crop out anywhere at Sentinel. This deep history might be entirely Triassic, based on the detrital zircon dates results and this borehole information. In correlating the exposed Mpandi Formation, then it means we might be missing most of the lower Elliot Formation and potentially the Molteno age equivalents.

Fossils

The Mpandi Formation at Sentinel Ranch had diverse taxa than it had been previously thought and they comprised both sauropodomorphs and the theropods. Sauropodomorphs were the most established during the late Triassic period in the Elliot Formation of the main Karoo Basin (Bordy *et al*, 2020). The fossils from the Mpandi Formation are dominated by Sauropodomorph bones, suggesting that they were also the most established fauna among the taxa at the time.

Sauropodomorphs are global biostratigraphic pointers in the latest Triassic and Early Jurassic (McPhee *et al*, 2017). Sauropodomorphs and Theropods also had a co-occurrence in the Elliot Formation of the main Karoo Basin in South Africa (Kitching and Raath, 1984; Olsen and Galton, 1984). Basing on the co-occurrence of Sauropodomorphs and the Theropods we can now corelate the Mpandi Formation with the Elliot Formation and hence constrain its age to late Triassic to Early Jurassic time span (Viglietti *et al*, 2020; Zondo, 2019; McPhee *et al*, 2017). The discovery of theropods material at the Wedding Hill is the first time theropods were found in the Tuli Basin. The co-occurrence of both sauropodomorphs and theropods in the Wedding Hill bonebed suggests that the Mpandi Formation could ecologically sustain a wide range of, and diverse fauna.

At the Sentinel Ranch, there were both small and medium-sized theropod dinosaurs, the small theropods were probable slightly bigger than the Syntarsus, judging by the size of the tibia bones. There were at least 2 individuals at the wedding Hill site. The discovery of the big sauropodomorph adds to the list that was reported during the reassessment of the fossil material that was historically collected from the Sentinel Ranch and the fossils that were being collected in the past few years. The tibia and fibula bones collected from the bonebed, measure approximately 650 mm in length. This size is outside the size range of *Massospondylus* and *Melanorosaurus* dinosaur size ranges, which suggest the bones belong to a different taxon.

As a general “rule” larger or robust sauropodomorph dinosaurs were thought to occur in the Lower Elliot Formation, whereas the gracile ones in the Upper Elliot Formation (Kitching and Raath, 1984; Bordy and Eriksson, 2015). Contrary to this general thought, it has been shown that robust taxa also occurred in the Upper Elliot Formation as well (McPhee *et al*, 2017). If the age of the Wedding Hill bonebed was estimated basing on that historical “rule”, its age would be like that of the Lower Elliot Formation beds, but this rule cannot be relied on since the findings by McPhee *et al*, (2017).

Both the sauropodomorphs and theropods bones collected from the wedding Hill and the Pimwe site are represented by various fragmented postcranial bones. Fossil bones from Pimwe were mostly coated in thin layer of haematite which gave them a brownish/reddish appearance (Rogers *et al*, 2004), This is like what was observed by researchers in some Elliot Formation fossil bones (Kitching and Raath, 1984). The bones from the Wedding Hill bonebed were preserved in a whitish carbonate mineral, likely calcite, which occurs in places around the farm. The mineral dissolves in hydrochloric acid. It can be inferred that these bones were preserved in beds that were saturated with carbonate mineral solutions.

The bones remained in subaerial conditions for some time after death before eventual burial, with some bones showing that they had already suffered some damage by the time they got buried. Sun cracks marks are also visible in some bones also indicating subaerial exposure for a long time in hot climatic environment, sun cracked bones are shown in Figure 7.1. This suggests that the bones were washed by turbulent flood waters from their places of death or from where they had been lying scattered on the earth surface and were deposited in pool that was formed by the subsiding flood water.

Figure 7.1. The diagram shows sun-cracked fossil bones from the Wedding Hill bonebed.

Detrital zircon dating of the Mpandi beds.

The LA- ICPMS analysis results for the detrital zircon samples gave the youngest age for the zircons as 199.2 ± 5.1 Ma which is maximum depositional age (MDA) of the zircon crystal hosting bed. This is an early Jurassic age given by a crystal from the old homestead site. Another early Jurassic age result came from a crystal that gave a MDA of 200.8 Ma, also from an old homestead sample. This could suggest that the beds were deposited in very short time-gaps of flood episodes. The samples did not yield many young zircons as was expected but rather Triassic ages. The expectation was to see the beds young upwards but it's not so with the Mpandi beds. There could possibly be a few reasons to explain this:

It could be that there was no volcanic ashfall with enough zircon crystals of young age during the deposition of the Mpandi beds.

It could be due to a lithological reason, it could be because the lithofacies were deposited rapidly through turbulent flows, creating fewer chances of preservation of the crystals.

It could be because the source of the volcano ashfall at that time was far from the Tuli Basin suggesting that the probability of having the ashfall reaching the Tuli Basin with enough zircons to be preserved was quite little.

The other possible reason could be related to the hiatus that occurred at the close of the Mpandi Formation deposition activities. This could mean that the young zircons that were reaching the Mpandi Formation during the hiatus could not be preserved since there was no deposition of sediments taking place.

It's possible that it could be because the gap between the samples is very small since the whole Mpandi sequence is very thin, there would be little difference in the ages of the samples.

The maximum depositional ages produced by the analysis range from the late Triassic to early Jurassic. This would suggest that the Mpandi Formation beds record the Triassic/Jurassic boundary and the end Triassic extinction event and other events that occurred during that time interval. At the Elliot Formation in the MKB, the Triassic Jurassic boundary (TJB) was constrained at 201.464 ± 0.004 Ma while the end Triassic extinction event (ETE) was constrained at 201.564 ± 0.015. The Central Atlantic Magnetic Province (CAMP) was constrained at 201.566 to 200.916 Ma. (Olsen *et al*.; Howard, 2023).

CHAPTER 8

Conclusion

The Mpandi Formation beds are dominated by fine-grained facies and sandstone facies that were deposited by fluvial systems that encountered occasional flooding episodes. Turbulent and high-powered flows resulted in the deposition of the pebbly sediments such as the infraformational conglomerates and breccias. The sequence of the Karoo sediments in the Tuli Basin was examined using the historical boreholes data. The sequence is very thin when in comparison with the main Karoo Basin. The sedimentology of the Mpandi Formation is like that of the Elliot Formation in the main Karoo Basin, and it can be interpreted as having been deposited under similar depositional environments.

With the use of the borehole data, the Mpandi Formation thickness was estimated at 190 metres of which 60 metres can be accessed as outcrops. At least 100 metres of the Mpandi Formation is totally unexposed. The LA-ICPMS analysis of detrital zircons dating, gave the maximum depositional age (MDA) from youngest zircon crystal with an age of 199.2 ± 5.1 Ma, Concordia diagrams and the raw data, suggest a late Triassic (Norian – Rhaetian) maximum depositional age for the beds at Sentinel.

The maximum depositional age is at the Triassic – Jurassic boundary as revealed by the combination of borehole and detrital zircon dates analysis. This means that the upper Mpandi possibly cuts right across the Upper Elliot / Lower Elliot Formation boundary. This research established the presence of theropods in the Mpandi Formation, suggesting that we are potentially seeing Triassic and Jurassic fauna at the two sites. The gap between the top of the Mpandi Formation and the Silcrete is large, this gap is evidenced by the presence of silcrete palaeosurface. A hiatus in time, of up to 14 million years is missing between the silcrete and the basalts.

References

Anderson, T., (2005). Detrital zircons as tracers of sedimentary provenance: limiting conditions from statistics and numerical simulation. Chemical Geology, Vol 216, issues 3-4, 25 March 2005, pp. 249-270.

Barrett, P. M., Chapelle, K. E.J., Staunton, C. K., Botha, J., Choiniere, J.N., (2019). Postcranial osteology of the neotype specimen of the *Massospondylus carinatus* Owen, 1854 (Dinosauria: Sauropodomorpha) from the Upper Elliot Formation of South Africa. Palaeontologia Africana, August 2019. 53; pp.114- 178.

Bordy, E. M., (2000). Sedimentology of the Karoo Supergroup in the Tuli Basin (Limpopo River Area, South Africa). A thesis submitted in fulfilment of the requirements of Docter of Philosophy of Rhodes University.

Bordy, E.M., Abrahams, M., Sharman, G.R., Viglietti, P.A., Benson, R.B.J., McPhee, B.W., Barrett, P.M., Sciscio, L., Condon, D., Mundil, R., Rademan, Z., Jinnah, Z., Clark, J.M., Suarez, C.A., Chapelle, K.E.J. and Choiniere, J.N., (2020). A chronostratigraphic framework for the upper Stormberg Group: Implications for the Triassic-Jurassic boundary in southern Africa. Earth-Science Reviews, [online] 203, p.103120. Doi: https://doi.org/10.1016/j.earscirev.2020.103120.

Bordy, E.M., Catuneanu, O., (2001). Sedimentology of the upper Karoo fluvial strata in the Tuli Basin, South Africa. Journal of African Earth Sciences 35, 605-629.

Bordy, E.M., Catuneanu, O., (2002). Sedimentology of the upper Karoo Aeolian strata (Early Jurassic) in the Tuli Basin, South Africa. Journal of African Earth Sciences 35, pp.301-314.

Bordy, E.M., Eriksson, P., (2015). lithostratigraphy of the Elliot formation (karoo supergroup), south Africa. South African Journal of Geology, 118(3), pp.311–316. Doi: https://doi.org/10.2113/gssajg.118.3.311.

Broderick, T.J., (1979). Explanation of the geological map of the country South of Nuanetsi, Nuanetsi and Beitbridge districts. [online] Available at: https://pascal-francis.inist.fr/vibad/index.php?action=getRecordDetail&idt=9555511 [Accessed 24 Mar. 2024].

Broom, R., (1911). On the remains of a Theropodous dinosaur from the Northern Transvaal. Transactions of the Geological society of South Africa*, v*ol xiv.

Catuneanu, O., Rubidge, B.S., Hancox, P.J.; Sequence analysis of the Ecca-Beaufort contact in the southern Karoo of South Africa. South African Journal of Geology (2000); 103 (1): pp.81–96. Doi: https://doi.org/10.2113/103.1.81

Catuneanu, O., Wopfner, H., Eriksson, P.G., Caincross, B., Rubidge, B.S., Smith, R.M.H., Hancox, P.J., (2005). The Karoo Basins of south-central Africa. Journal African Earth Sciences 43, pp.211-253.

Chinoda, G., Matura, N., Moyce, W. and Owen, R., (2009). Baseline Report on the Geology of the Limpopo Basin Area, a contribution to the Challenge Program on Water and Food Project 17 "Integrated Water Resource Management for Improved Rural Livelihoods: Managing risk, mitigating drought and improving water productivity in the water scarce Limpopo Basin*"*. WaterNet Working Paper 7. WaterNet, Harare.

Claire Peyre de Fabrègues, Ronan Allain. New material and revision of *Melanorosaurus thabanen-sis*, a basal sauropodomorph from the Upper Triassic of Lesotho. Peer. J, (2016), 4, pp. e1639.10.7717/peerj.1639. hal-01285015.

Cooper, M.R., (1981). The prosauropod dinosaur *Massospondylus carinatus Owen* from Zimbabwe: its biology, mode of life and phylogenetic significance. Occasional Papers of The National Museums and Monuments *6,10.*

Couts, S.D., Mathews, A.W., Hubbard, M. S., (2019). Assessment of the widely used methods to derive depositional ages from detrital zircon populations. Geoscience Frontiers, Vol 10, Issue 4, July 2019, pp. 1421-1435.

Davis, D.W., (2023). U–Pb geochronology: its development and importance in Canada. Canadian Journal of Earth Sciences, 60(4), pp.388–400. Doi: HTTPs://doi.org/10.1139/cjes-2023-0009.

Glover, P.W.J. and Bormann, P., (2007). The characterization of trough and planar crossbedding from borehole image logs. Journal of Applied Geophysics, 62(2), pp.178–191. Doi: https://doi.org/10.1016/j.jappgeo.2006.11.001.

Howard, B. L., (2023). Maximum Depositional Age Analysis using Paired LA-ICP-MS and CA-ID-TIMS Detrital Zircon U-Pb Geochronology. Graduate Theses and Dissertations Retrieved from https://scholarworks.uark.edu/etd/5182.

Khoza, D., Jones, A.G., Muller, M.R., Evans, R.L., Webb, S.J. and Miensopust, M., (2013). Tectonic model of the Limpopo belt: Constraints from magnetotelluric data. Precambrian Research, 226, pp.143–156. Doi: HTTPs://doi.org/10.1016/j.precamres.2012.11.016.

Khoza, T.D., Jones, A.G., Muller, M.R., Evans, R.L., Miensopust, M.P. and Webb, S.J., (2013b). Lithospheric structure of an Archean craton and adjacent mobile belt revealed from 2-D and 3-D inversion of magnetotelluric data: Example from southern Congo craton in northern Namibia. Journal of Geophysical Research: Solid Earth, 118(8), pp.4378–4397. Doi: HTTPs://doi.org/10.1002/jgrb.50258.

Kitching, J.W., Raath, M.A., (1984). Fossils from the Elliot and Clarens Formations (Karoo sequence) of the North-eastern Cape, Orange Free State and Lesotho, and a suggested bio-zonation based on tetrapods. Palaeontologia Africana., 25. Pp.111-125.

Langer, M. C., McPhee, B.W., Marsola, J.C. A., Silva, L. R., Cabreira, S. F., (2019). Anatomy of the dinosaur Pampadromaeus barberenai (Saurischia – Sauropodomorph) from the Late Triassic Santa Maria Formation of southern Brazil. Plos ONE 142(2) 1- 64.

Linol, B., de Wit, M.J., Kasanzu, C.H., da Silva Schmitt, R., Corrêa-Martins, F.J., Assis, A., (2016). Correlation and Paleogeographic Reconstruction of the Cape-Karoo Basin Sequences and Their Equivalents Across Central West Gondwana. In: Linol, B., de Wit, M. (eds) Origin and Evolution of the Cape Mountains and Karoo Basin. Regional Geology Reviews. Springer, Cham. https://doi.org/10.1007/978-3-319-40859-0_18

Lister, J.R., (1987). Density-driven Flows in Geological Fluid Mechanics, Cambridge University.

McCoy, S., Coe, J., Kean, J., Tucker, G., Staley, D. and Wasklewicz, T., (2011) "Observations of debris flows at Chalk Cliffs, Colorado, USA: Part 1, In situ measurements of flow dynamics, tracer particle movement and video imagery from the summer of 2009", Italian journal of engineering geology and environment, pp. 715–726. Available at: https://rosa.uniroma1.it/rosa02/engineering_geology_environment/article/view/1310 (Accessed: 24 March 2024).

McPhee, B.W., Bordy, E.M., Sciscio, L., Choiniere, J.N., (2017). The Sauropodomorph Biostratigraphy of the Elliot Formation of southern Africa: Tracking the evolution of Sauropodomorpha across the Triassic- Jurassic boundary. Acta Paleontologica Polonica 62(3), pp.441- 465.

McPhee, B.W., Choiniere, J.N., (2017). The osteology of *Pulanesaura* ecolium: Implications for the inclusivity of sauropoda (Dinosauria). Zoological Journal of the Linnean Society, 2017, pp.1-32.

Miall, A.D., (2006). Methods of Architectural-Element Analysis. In: The Geology of Fluvial Deposits. Springer, Berlin, Heidelberg. https://doi.org/10.1007/978-3-662-03237-4_4

Miall, A., (2013a). Analysis of Fluvial Depositional Systems. [online] Available at: https://hmtg.itny.ac.id/wp-content/uploads/2019/01/1981.-Analysis-of-Fluvial-Depositional-Systems-miall-1981.pdf.

Miall, A.D. and Miall, A.D., (1982). Analysis of fluvial depositional systems.

Miall, A. and Miall, A., (2014). The Nature and Purpose of This Book. Fluvial Depositional Systems, pp.1-8.

Molyneux, A.J.C., (1903). The sedimentary deposits of Southern Rhodesia. *Q.* Jl geol. Soc. Lond., 59, pp.266-291.

Molyneux, A.J.C., 1908. On the correlation of the Karroo System in Rhodesia. Rep. S. Afr. Ass. Advmt Sci., 6(1), 21.

Molyneux, A.J.C. and Mennell, F.P., (1905). Dwyka conglomerate from Tuli district. Proc. Trans. Rhod. scient. Ass., 5(2), pp.10-11.

Müller, R.T., Langer, M.C. and Dias-da-Silva, S., (2018). An exceptionally preserved association of complete dinosaur skeletons reveals the oldest long-necked sauropodomorphs. Biology Letters, 14(11), p.20180633. Doi: HTTPs://doi.org/10.1098/rsbl.2018.0633.

Munyikwa, D., (1997). Faunal analysis of Karoo-aged sediments in the Northern Limpopo Valley, Zimbabwe. Arnoldia Zimbabwe 10, pp.129- 140.

Olsen, P.E., Galton, P.M., (1984). A Review of the reptile and amphibian assemblages from the Stormberg of southern Africa, with special emphasis on the footprints and the age of the Stormberg. Palaeont. Afr., 25, pp.87-110.

Olsen, P.E., Shubin, N.H., Anders, M.H., (2017). New Early Jurassic Tetrapod Assemblages Constrain Triassic- Jurassic Tetrapod Extinction Event. *S*cience 237 (4818), pp.1025- 1029.

Reading, H.G., (2001). Clastic facies models, a personal perspective. Bulletin of the Geological Society of Denmark, 48, pp.101–115. Doi: HTTPs://doi.org/10.37570/bgsd-2001-48-05.

Robertson, I., (1967). Geological report. Rhod. Sch*.* Explor. Soc. (Matabeleland Branch) 17th Exped, pp.34-9.

Rogers, R.C., Raymond, R. and Karl, R. (n.d.). Abstract: Character and origin of the Mpandi silcrete (Early Jurassic?), Limpopo Valley, Zimbabwe (GSA Annual Meeting, Novembe*r 5-8, 2001)*. [online] gsa.confex.com. Available at: https://gsa.confex.com/gsa/2001AM/webprogram/Paper26393.html [Accessed 24 Mar. 2024].

Rogers, R.R., Rogers, K.C., Munyikwa, D., Terry, R.C., Singer, B.S., (2004). Sedimentology and taphonomy of the upper Karoo- equivalent Mpandi Formation in the Tuli Basin of Zimbabwe, with a new $^{40}Ar/^{39}Ar$ age for the Tuli basalts. Journal of African Earth Sciences 40, pp.147- 161.

Schoene, B., (2014). U–Th–Pb Geochronology. Treatise on Geochemistry, pp.341–378. Doi: HTTPs://doi.org/10.1016/b978-0-08-095975-7.00310-7.

Sereno, P.C., ElShafie, S.J., (2013). A New Long-Necked Turtle, *Laganemys tenerensis* (Pleurodira: Araripemydidae), from the Elrhaz Formation (Aptian–Albian) of Niger. In: Brinkman, D., Holroyd, P., Gardner, J. (eds) Morphology and Evolution of Turtles. Vertebrate Paleobiology and Paleoanthropology. Springer, Dordrecht. https://doi.org/10.1007/978-94-007-4309-0_14

Shubin, N.H., Sues, H., (1991). Biogeography of early Mesozoic continental tetrapods: patterns and implications. Paleobiology 17(3), pp.214- 230.

Smith, F. A., Payne, J. L., Heim, N. A., Balk, M. A., Finnegan, S., Kowalewski, M., Lyons, S. K., McClain, C. R., McShea, D. W., Novack-Gottshall, P. M., Anich, P. S., Wang, S. C., (2016). Body Size Evolution Across the Geozoic. Ann.Rev. Earth Planet.Scie.2016, 44: pp.523-53.

Sues, H.D., Olsen, P.E., (2015). Stratigraphic and temporary context and faunal diversity of Permian- Jurassic continental tetrapod assemblages from the Fundy rift basin, Eastern Canada. Atlantic Geology 51, pp.139-205.

Thompson, A.O., (1975). The Karoo rocks in the Mazunga area, Beitbridge District. Rhodesia Geological Survey, Short Report No. 40. Harare.

Vail, J. R., Snelling, N. J., and Rex, D. C., (1969). Pre-Katangan geochronology of Zambia and adjacent parts of Central Africa. Canad, J. Earth Sci., 5, pp.621-628

Viglietti, P.A., (2020). Biostratigraphy of the Daptocephalus Assemblage Zone (Beaufort Group, Karoo Supergroup), South Africa. South African Journal of Geology, 123(2), pp.191–206. Doi: HTTPs://doi.org/10.25131/sajg.123.0014.

Watkeys, M.K., and Sweeny, R.J., (1990). A possible link between Mesozoic lithospheric architecture and Gondwana flood basalts. Journal Of African Earth Sciences, 10(4), p.88. Doi: HTTPs://doi.org/10.1016/0899-5362(90)90037-f.

Yates, A.J.P., Neumann, F.-J., Uken, R., Smith, A.M., Guastella, L. and Cawthra, H.C., (2012). Sedimentation on the narrow (8 km wide), oceanic current-influenced continental shelf off Durban, Kwazulu-Natal, South Africa. Sedimentation on the Narrow (8 Km wide), Oceanic current-influenced Continental Shelf off Durban, Kwazulu-Natal, South Africa, 323-325, pp.107–122. Doi: HTTPs://doi.org/10.1016/j.margeo.2012.08.001.

Yates, A.M., Wedel, M.J. and Bonnan, M.F., (2012). The Early Evolution of Postcranial Skeletal Pneumaticity in Sauropodomorph Dinosaurs. Acta

Palaeontologica Polonica, 57(1), pp.85–100. Doi: HTTPs://doi.org/10.4202/app.2010.0075.

Zamanian, H., Ahmadnejad, F. and Zarasvandi, A., (2016). Mineralogical and geochemical investigations of the Mombi bauxite deposit, Zagros Mountains, Iran. Geochemistry, 76(1), pp.13–37. Doi: HTTPs://doi.org/10.1016/j.chemer.2015.10.001.

Zondo, M., (2019). Palaeontology of the new Tuli Basin fossil sites in Zimbabwe. Honours Degree Research project, University of the Witwatersrand, Johannesburg South Africa.

APPENDECES

Detrital zircon raw data

Appendix A contains raw data from LA-ICPMS analysis of zircons from Wedding Hill site. (attached as a separate file)

B. Appendix B contains raw data from LA-ICPMS analysis of zircons from all tested sites. (attached as a separate file)

C. Appendix C is a collection of various post cranial elements collected from the Wedding Hill site; they are associated with the fossils collected from the site.